JEM Journal of Experimental Medicine

ARTICLE

BAFFR controls early memory B cell responses but is dispensable for germinal center function

Angelica W.Y. Lau[1], Vivian M. Turner[1], Katherine Bourne[1], Jana R. Hermes[1], Tyani D. Chan[1,2], and Robert Brink[1,2]

The TNF superfamily ligand BAFF maintains the survival of naive B cells by signaling through its surface receptor, BAFFR. Activated B cells maintain expression of BAFFR after they differentiate into germinal center (GC) or memory B cells (MBCs). However, the functions of BAFFR in these antigen-experienced B cell populations remain unclear. Here, we show that B cell–intrinsic BAFFR does not play a significant role in the survival or function of GC B cells or in the generation of the somatically mutated MBCs derived from them. Instead, BAFF/BAFFR signaling was required to generate the unmutated, GC-independent MBCs that differentiate directly from activated B cell blasts early in the response. Furthermore, amplification of BAFFR signaling in responding B cells did not affect GCs or the generation of GC-derived MBCs but greatly expanded the GC-independent MBC response. Although BAFF/BAFFR signaling specifically controlled the formation of the GC-independent MBC response, both types of MBCs required input from this pathway for optimal long-term survival.

Introduction

Humoral immunity following infection or vaccination depends on the proliferative expansion of rare antigen-specific B cells from the naive repertoire and their subsequent differentiation into antibody-secreting plasma cells (PCs), somatically mutating germinal center (GC) B cells, or quiescent memory B cells (MBCs). Within 1–2 d of antigen challenge, activated B cells form into a population of rapidly dividing, undifferentiated B cell blasts driven by CD40 ligand (CD40L) and other stimuli derived from cognate CD4$^+$ T helper cells (Chan et al., 2009; Garside et al., 1998; Reif et al., 2002). After 3–4 d, these early B cell blasts differentiate into either (1) short-lived extrafollicular plasmablasts that provide the initial wave of secreted antibody production (MacLennan et al., 2003) or (2) follicular GC B cells that continue to proliferate, undergo somatic hypermutation (SHM) of their Ig variable region genes and selection for variants with increased affinity for antigen (Victora and Nussenzweig, 2012). GC B cells also depend on CD40L supplied by ongoing interactions with specialized T follicular helper (Tfh) cells localized within the GC and ultimately differentiate into either PCs that secrete high-affinity antibodies or affinity-matured MBCs that can mediate rapid recall responses upon antigen rechallenge (Suan et al., 2017b).

Although it is well established that PCs can emerge independent of the GC response (MacLennan et al., 2003), only recently has it been appreciated that the same is also true for MBCs (Takemori et al., 2014; Tarlinton and Good-Jacobson, 2013). Thus, in addition to GC B cells and plasmablasts, early B cell blasts can also differentiate directly into quiescent MBCs without the requirement for prior passage through the GC (Chan et al., 2009; Kaji et al., 2012; Takemori et al., 2014; Taylor et al., 2012; Toyama et al., 2002). These early, GC-independent MBCs are frequently unswitched (IgM$^+$) but can also be IgG$^+$ due to the onset of class-switch recombination soon after B cell activation and before GC B cell differentiation (Chan et al., 2009; Pape et al., 2003; Taylor et al., 2012; Toellner et al., 1996). GC-independent MBCs characteristically lack somatic mutations in their Ig variable region genes and also have not undergone the affinity-based selection typical of GC-derived MBCs. As a consequence, GC-independent MBCs are thought to provide a pool of broad specificities that may help counter the emergence of mutant or related pathogens that may escape recognition by the more specific GC-dependent MBCs (Takemori et al., 2014; Tarlinton and Good-Jacobson, 2013).

Although B cells responding to T-dependent antigen depend on signals delivered through cell surface CD40 (TNFRSF5), the survival of naive resting B cells instead requires triggering of an alternative member of the TNF receptor (TNFR) superfamily, BAFFR (TNFRSF13C). Mature, naive B cells fail to survive in the absence of either BAFFR or its specific ligand BAFF (TNFSF13B; Gross et al., 2001; Schiemann et al., 2001; Thompson et al.,

[1]Immunology Division, Garvan Institute of Medical Research, Darlinghurst, New South Wales, Australia; [2]St. Vincent's Clinical School, University of New South Wales, Darlinghurst, New South Wales, Australia.

Correspondence to Robert Brink: r.brink@garvan.org.au.

2001), with the result being that secondary lymphoid tissues contain follicles greatly reduced in size and with compromised development of stromal elements such as follicular dendritic cells (Rahman et al., 2003; Vora et al., 2003). Mice lacking either BAFFR or BAFF initiate GC responses following challenge with T-dependent antigen, but these rapidly attenuate and are not sustained (Rahman et al., 2003; Sasaki et al., 2004; Shulga-Morskaya et al., 2004; Vora et al., 2003). It remains unclear whether this is due to the lack of BAFFR signaling in responding GC B cells or to extrinsic issues such as impaired development of stromal elements. Indeed, the role of BAFF/BAFFR signaling in regulating the fate of GC B cells remains undefined. In contrast, it has been shown in two separate studies that the depletion of BAFF efficiently removes naive B cells without impacting MBC numbers greatly (Benson et al., 2008; Scholz et al., 2008).

To determine the B cell–intrinsic functions of BAFF/BAFFR signaling during a T-dependent response, we employed a variety of complementary approaches to circumvent the previously confounding issues of impaired B cell development and compromised follicular microenvironment associated with the global absence of either one of this ligand–receptor pair. Although BAFFR expression was maintained throughout GC B cell and MBC differentiation, the selection, survival, and persistence of GC B cells proceeded normally in B cells lacking BAFFR, as did the production of somatically mutated and affinity-matured MBCs derived from GC B cell precursors. In contrast, the GC-independent generation of both switched and unswitched MBCs early in the response required both cell-intrinsic BAFFR expression and availability of BAFF. Strikingly, augmentation of BAFFR signaling also selectively expanded the GC-independent MBC pool. Taken together, these data indicate a specific requirement for BAFF/BAFFR signaling in controlling the pool of MBCs that maintain broad antigen specificity.

Results

T cell–derived BAFF does not significantly impact the GC response

Although there are only limited data on the role of BAFF/BAFFR signaling in the GC, one previous study of responses to OVA-conjugated 4-hydroxy-3-nitrophenylacetyl indicated that Tfh cell–derived BAFF may regulate the selection of high-affinity B cells within the GC (Goenka et al., 2014). To determine if this finding is generally applicable, we first performed a similar investigation of responses against a mutant form of the hen egg lysozyme protein (HEL^{3X}; Paus et al., 2006) conjugated to sheep RBCs (HEL^{3X}-SRBC). Two groups of mixed bone marrow (BM) chimeric mice were established on a C57BL/6 ($CD45.2^+$) background in which T cells were either WT or BAFF deficient (BAFFΔ; Fig. 1 A). Reconstituted chimeras were injected i.v. with B cells from the SW_{HEL} mice, which express the anti-HEL specificity of the HyHEL10 mAb (Phan et al., 2003), together with HEL^{3X}-SRBC antigen (Fig. 1 A). Donor SW_{HEL} B cells, detectable by flow cytometry in recipient mice as $CD45.1^+CD45.2^-$ (Fig. S1 A), undergo T-dependent proliferative expansion, Ig class switching, and SHM in these responses and differentiate into GC B cells as well as GC-dependent and GC-independent PCs and MBCs (Chan et al., 2009; Kräutler et al., 2017; Paus et al., 2006; Phan et al., 2003, 2006; Suan et al., 2017a). Donor-derived SW_{HEL} GC B cells also undergo affinity maturation to HEL^{3X}, primarily through the acquisition of the Y53D substitution in the HyHEL10 heavy chain variable region but also complemented by S31R and Y58F substitutions after days 9–10 of the response (Chan et al., 2012; Paus et al., 2006).

Detailed analysis of the responses of SW_{HEL} B cells failed to identify a significant difference between those supported by T cells that could or could not express BAFF. Class switching to IgG1 and the size of the GC B cell and MBC responses did not vary between chimeras containing WT versus BAFFΔ T cells on either day 14 or day 21 after antigen challenge (Fig. 1, B and C). Affinity maturation, as measured by the proportion of $IgG1^+$ GC B cells capable of binding a low concentration (50 ng/ml) of HEL^{3X} (Paus et al., 2006), was similar in responses that took place within the two sets of chimeras (Fig. S1, B and D), as was the fraction of high-affinity cells within the $IgG1^+$ MBC compartment (Fig. S1, C and E). Accordingly, the frequency and pattern of Ig heavy chain SHM events among $IgG1^+$ GC B cells on day 21 of the response, including the frequencies of the Y53D, S31R, and Y58F substitutions that bestow increased affinity for HEL^{3X}, did not vary between chimeras containing WT or BAFFΔ T cells (Fig. 1 D). Although a slightly lower titer of anti-HEL^{3X} serum IgG1 was measured in chimeras containing BAFFΔ T cells, this was not statistically significant (Fig. 1 E). Taken together, these data indicate that Tfh cell–derived BAFF has minimal influence over GC B cell responses in this system.

BAFF is required to support a GC-independent MBC response

Because we did not find a prominent role for Tfh cell–derived BAFF in regulating T-dependent B cell responses, we next undertook a more fundamental examination of the role(s) of BAFF and BAFFR in this process. First, WT mice were challenged with SRBCs, and their spleen cells were analyzed for surface BAFFR expression 9 d later. Both the $IgG1^+$ GC B cells and MBCs generated in these responses were confirmed to express levels of BAFFR similar to those found on naive follicular B cells (Fig. S2, A and B) and so to have the potential to respond to BAFF.

We next used mice that lacked expression of either BAFF ($Tnfsf13b^{-/-}$ = BAFFΔ) or BAFFR ($Tnfrsf13c^{-/-}$ = BAFFRΔ). Flow cytometric analysis of unimmunized animals confirmed the specific absence of BAFFR from BAFFRΔ mice (Fig. S2 C) and reduced numbers of splenic leukocytes and B cells in both BAFFΔ and BAFFRΔ mice (Fig. S2 D). WT SW_{HEL} B cells (expressing BAFFR) were transferred into WT, BAFFΔ, and BAFFRΔ mice, then challenged with HEL^{3X}-SRBC (Fig. 2 A), and splenic responses were analyzed on day 14 by flow cytometry. As expected, donor-derived GC responses in BAFFΔ and BAFFRΔ recipients were reduced compared with WT recipients (Fig. 2, B and C), presumably due to the impaired development of follicular structures associated with the paucity of mature B cells in these animals (Rahman et al., 2003; Vora et al., 2003). Nevertheless, affinity maturation progressed efficiently among the SW_{HEL} GC B cells in both BAFFΔ and BAFFRΔ recipients (Fig. 2 D), as did SHM and positive selection for Y53D-containing GC B cells (Fig. 2 E).

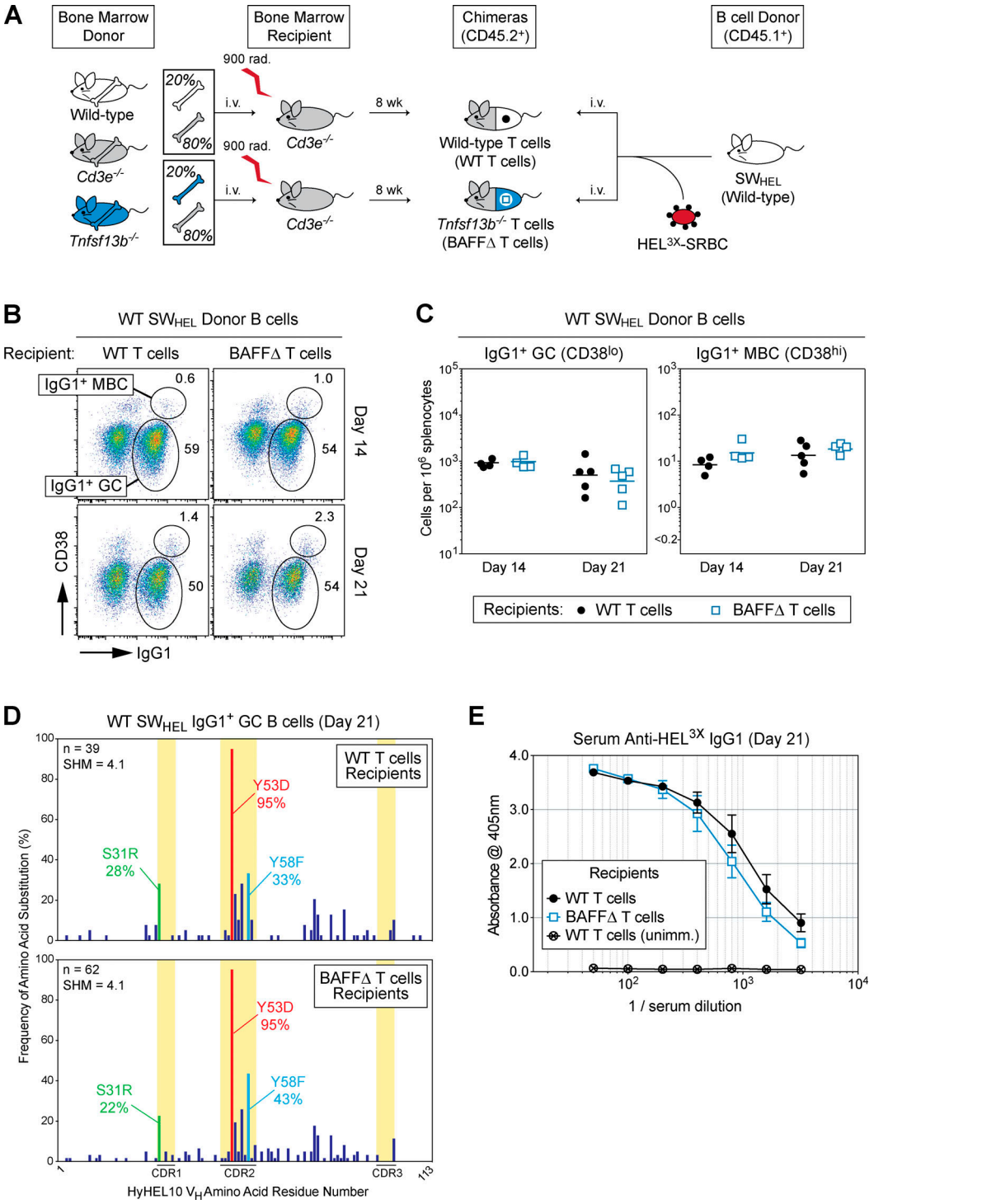

Figure 1. **T cell–derived BAFF does not significantly impact the GC response. (A)** WT T cell or BAFFΔ T cell chimeras were generated by mixing BM from *Cd3e*$^{-/-}$ with WT or BAFFΔ mice in a ratio of 80% *Cd3e*$^{-/-}$ to 20% WT BM or 80% *Cd3e*$^{-/-}$ to 20% *Tnfsf13b*$^{-/-}$ BM mixtures, respectively. Mixed BM were injected i.v. into lethally irradiated *Cd3e*$^{-/-}$ mice and allowed to reconstitute for 6–8 wk, and SW_{HEL} B cells were adoptively transferred and challenged with HEL^{3X}-SRBC. WT T cells (black dots) or BAFFΔ T cells (blue squares) chimeric recipients were antigen boosted on day 4, and T-dependent B cell responses were examined on days 14 and 21. **(B)** Flow cytometric analysis of donor-derived SW_{HEL} B cells (CD45.1$^+$, CD45.2$^-$, B220$^+$), with gates showing IgG1$^+$ GC (IgG1$^+$, CD38^{lo}) and IgG1$^+$ MBCs (IgG1$^+$, CD38^{hi}) in WT T cell and BAFFΔ T cell chimeric recipients on day 14 (top) and day 21 (bottom). **(C)** Enumeration of SW_{HEL} IgG1$^+$ GC B cells (left) and IgG1$^+$ MBCs (right) in WT T cell and BAFFΔ T cell chimeric recipients on days 14 and 21. Enumerated data were analyzed using an unpaired Student's *t* test with Welch's post hoc correction; no statistical significance was found. **(D)** SHM analysis of day 21 single-cell–sorted SW_{HEL} IgG1$^+$ GC B cells in WT T (top) and BAFFΔ T cell (bottom) chimeric recipients. Skyscraper plot shows percentage of mutation at each amino acid residue of SW_{HEL} B cell (HyHEL10) heavy chain variable region V_H10. CDR1, CDR2, and CDR3 are highlighted in yellow. High-affinity mutations to HEL^{3X}: Y53D in red; additional affinity-increasing mutations: Y58F in blue, S31R in green. n, number of clones analyzed; SHM, average number of mutations per clone. SHM data represent five pooled recipient mice from one experiment and are representative of two independent experiments. **(E)** Titration of day 21 HEL^{3X}-binding serum IgG1 antibodies detected in WT

T cell and BAFFΔ T cell chimeric recipients. Serum from unimmunized WT mice (crossed circle) was used as a negative control. ELISA data show geometric mean derived from five individual mice from one experiment and are representative of two independent experiments.

Strikingly, SW_{HEL} donor-derived IgG1$^+$ MBC responses were absent from BAFFΔ but not BAFFRΔ recipients (Fig. 2, B and C). Because both types of recipients sustained equivalent GC B cell responses and ostensibly differ only in the presence or absence of BAFF expression, these results point to a potent role for BAFF in the control of MBC responses. Interestingly, the vast majority of SW_{HEL} donor-derived IgG1$^+$ MBCs generated in BAFFRΔ recipients possessed uniformly low affinity for HEL^{3X} (Fig. 2, D and F) and almost exclusively lacked SHM of their Ig heavy chain variable region (Fig. 2 E), indicating that they represented predominantly unmutated, GC-independent MBCs. The size of the GC-independent MBC response was actually increased on day 14 in BAFFRΔ versus WT recipients (Fig. 2, D–F), likely due to the increased levels of BAFF present in these B-lymphopenic animals (Kreuzaler et al., 2012). Thus, the action of BAFF on activated B cells appears to be important for supporting and potentially regulating the size of GC-independent MBC responses.

GC responses progress normally in the absence of BAFFR expression

To examine the role of cell-intrinsic BAFFR in T-dependent B cell responses, CD45.1 congenic SW_{HEL} mice were bred onto the BAFFRΔ background, and HEL-binding B cells from these mice were challenged with HEL^{3X}-SRBC in WT (CD45.2$^+$) recipient animals (Fig. 3 A). HEL-binding B cells from SW_{HEL}.BAFFRΔ mice were confirmed to lack BAFFR expression (Fig. S3 A) but, unlike HEL-binding B cells from WT SW_{HEL} mice, were comprised almost exclusively of CD21/35^{lo}, CD23^{lo}, CD93^{hi} immature B cells (Fig. S3 B). Thus, to directly compare the responses of B cell populations that differed only in terms of BAFFR expression, adoptive transfer experiments were performed using WT SW_{HEL} and SW_{HEL}.BAFFRΔ donor spleen cells that had first been depleted of all mature B cells (Fig. 3 A and Fig. S3, A and B). Using this strategy, BAFFR expression by responding B cells was found to have no detectable impact on the overall magnitude of the GC response (Fig. 3, B and C) or upon switching to IgG1 (Fig. S3 C). Affinity maturation as assessed by accumulation of GC B cells with high affinity for HEL^{3X} was also unaffected on both days 12 and 21 of the response (Fig. S3, C and D), and both the rate of SHM and selection for the Y53D, S31R, and Y58F substitutions remained unchanged in the absence of BAFFR expression (Fig. 3 D and Fig. S3 E). Finally, on both days 12 and 21 of the response, the production of affinity-matured serum IgG1 antibodies directed against HEL^{3X} was indistinguishable, regardless of whether responding GC B cells expressed BAFFR (Fig. S3, F and G). Thus, the absence of BAFFR from responding GC B cells had no detectable effect on either the size or the normal function of the GC response.

GC-independent MBC responses are impaired in the absence of BAFFR expression

In contrast to the normal GC responses mounted by BAFFR-deficient SW_{HEL} B cells, the numbers of IgG1$^+$ MBCs they produced were found to be significantly lower than those derived from the control, immature WT SW_{HEL} donor B cells on both days 12 and 21 of the response (Fig. 3 C). Examination of SHM in the IgG1$^+$ MBC populations indicated that the absence of BAFFR expression disproportionately affected the contribution of unmutated, GC-independent MBCs to the response as opposed to the somatically mutated, GC-dependent MBCs (Fig. 3 E). Consistent with this, the numbers of low-affinity but not high-affinity IgG1$^+$ MBCs were reduced by almost 10-fold on day 12 of the response of BAFFR-deficient SW_{HEL} B cells (Fig. 3, F and G). A similar bias in the impact of BAFFR deficiency was evident on day 21 of the response, although, by this time point, a reduction in GC-dependent IgG1$^+$ MBCs derived from the SW_{HEL}.BAFFRΔ B cell response was also apparent (Fig. 3, F and G). Thus, BAFFR expression on responding B cells plays an important role in regulating the magnitude of the MBC responses and is particularly important for establishing the GC-independent MBC pool.

Acute BAFF depletion preferentially reduces the GC-independent MBC response

Because BAFF is the only known ligand for BAFFR, our results predicted that the presence of BAFF as well as B cell–intrinsic BAFFR expression should be required to establish GC-independent MBC responses. To test this, we asked whether acute depletion of BAFF in an otherwise WT setting (i.e., donor CD45.1$^+$ SW_{HEL}.WT B cells and WT CD45.2$^+$ recipients) would result in the abrogation of the GC-independent MBC response. Although our previous experiments had focused on IgG1$^+$, CD38^{hi} B cells due to their unequivocal status as antigen-experienced MBCs, in this experiment, we sought to identify both switched and unswitched (IgM$^+$) MBCs. To achieve this, recipient mice were placed on BrdU-containing drinking water from 2 d before donor cell and HEL^{3X}-SRBC immunization and were maintained on BrdU water for 4 d after antigen challenge, so that all cells undergoing cell division during this time would incorporate BrdU into their DNA (Fig. 4 A). We reasoned that B cells that had proliferated during the early phase of the response and differentiated soon after into quiescent, GC-independent MBCs could be identified as those that remained BrdU$^+$ 10–17 d after the cessation of BrdU administration (days 14–21 of the response).

To validate this approach, we first analyzed donor-derived CD38^{hi} B cells from days 4–21 of the response (Fig. 4 A). On day 4, ∼95% of donor-derived B cells were CD38^{hi} and could be divided into BrdU$^+$ blasts expressing the HEL-binding BCR and BrdU$^-$ naive B cells that did not express this BCR despite originating from the SW_{HEL} donor (Fig. 4 B; Phan et al., 2003). By day 7, many HEL-binding B cells had undergone differentiation into CD38^{lo} GC B cells and become BrdU$^-$ due to the multiple cell divisions they had undergone in the 3 d since BrdU withdrawal (Fig. 4 B). However, a significant proportion of CD38^{hi} B cells remained BrdU$^+$ on day 7, presumably having become quiescent since the cessation of BrdU administration (Fig. 4 B). CD38^{hi} MBCs with high affinity for HEL^{3X} began to appear on day 7 and

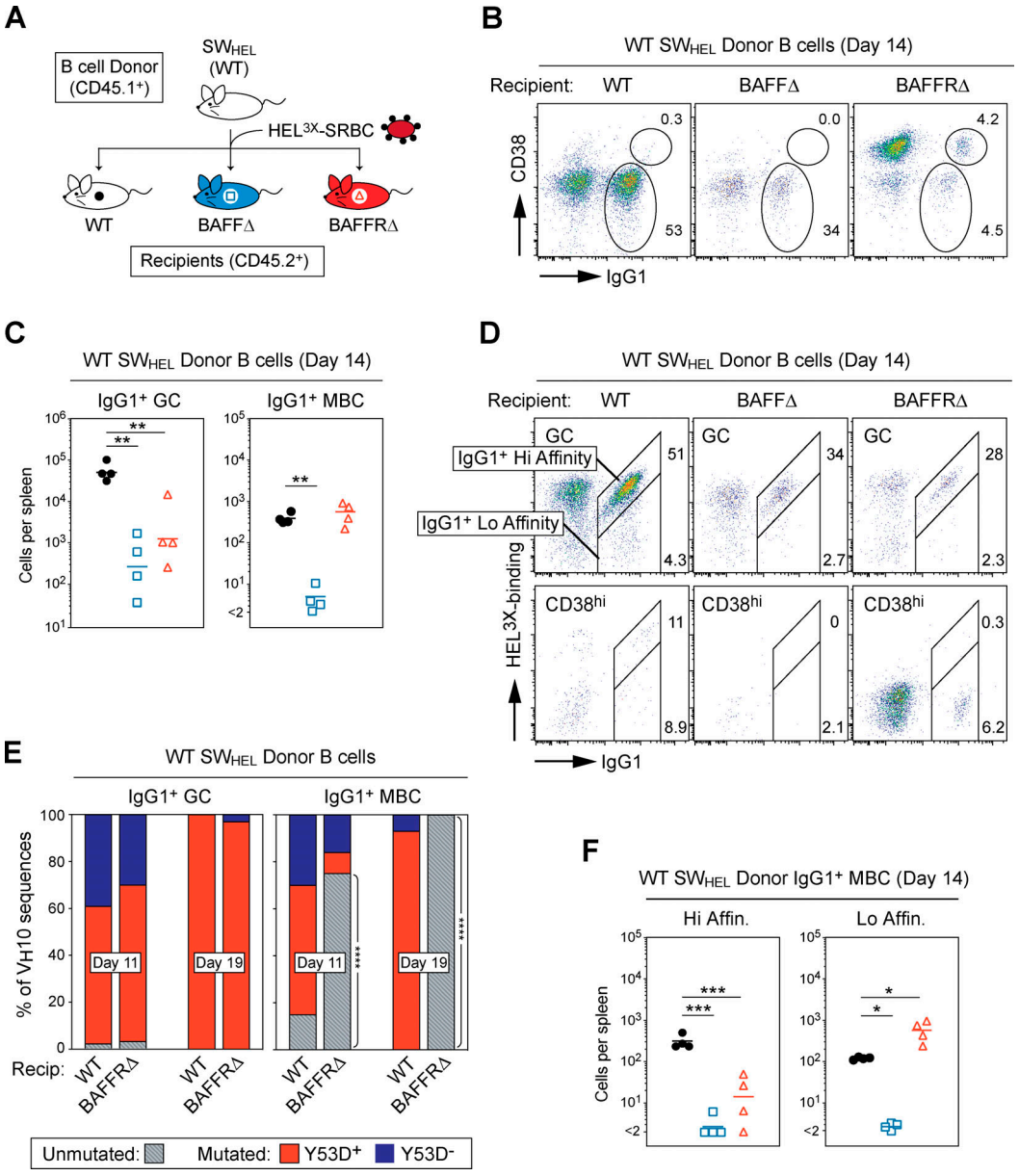

Figure 2. **BAFF is required to support a GC-independent MBC response. (A)** Transfer strategy to examine cell-extrinsic impact of BAFF or BAFFR deficiency on T-dependent responses of WT B cells. WT SW_{HEL} B cells were adoptively transferred into WT (black dots), BAFFΔ (blue squares), and BAFFRΔ (red triangles) recipient mice and challenged with HEL^{3X}-SRBC. Recipient mice were antigen boosted on day 4 and harvested on day 14. **(B)** Flow cytometric analysis of donor-derived WT SW_{HEL} B cells ($CD45.1^+$, $CD45.2^-$, $B220^+$) in WT, BAFFΔ, and BAFFRΔ recipients, with gates showing $IgG1^+$ GC B cells ($IgG1^+$, $CD38^{lo}$) and $IgG1^+$ MBCs ($IgG1^+$, $CD38^{hi}$) on day 14. **(C)** Enumeration of SW_{HEL} $IgG1^+$ GC B cells (left) and $IgG1^+$ MBCs (right) in WT, BAFFΔ, and BAFFRΔ recipients on day 14. **(D)** Flow cytometric analysis of SW_{HEL} GC B cells ($B220^{hi}$, $CD38^{lo}$; top) and $CD38^{hi}$ B cells ($B220^{hi}$, $CD38^{hi}$; bottom) on day 14, with gates showing $IgG1^+$ HEL^{3X}-binding high- and low-affinity GC and MBC compartments in WT, BAFFΔ, and BAFFRΔ recipients. Flow data in B and D represent five replicate mice from one experiment and are representative of two independent experiments. **(E)** SHM analysis of days 11 and 19 single-cell–sorted SW_{HEL} $IgG1^+$ GC B cells and $IgG1^+$ MBCs in WT and BAFFRΔ recipients. Proportion of SW_{HEL} $IgG1^+$ GC (left) and $IgG1^+$ MBC (right) clones with no mutation (gray), with high-affinity Y53D mutation (red) or low-affinity without Y53D mutation (blue) in SW_{HEL} B cell (HyHEL10) heavy chain variable region V_H10. SHM data represent five pooled recipient mice from one experiment and are representative of two independent experiments. Numbers of clones analyzed (n, from left to right) = 44, 37, 43, 34, 46, 43, 41, 33. SHM data were analyzed using the χ^2 test (CI = 99%), and statistical significance in frequency of unmutated clones is denoted by P values; ****, $P < 0.0001$. **(F)** Enumeration of HEL^{3X}-binding high-affinity (left) and low-affinity (right) $IgG1^+$ MBCs in WT, BAFFΔ, and BAFFRΔ recipient mice on day 14. Enumerated data in C and F were analyzed with unmatched one-way ANOVA with multiple comparisons conducted using Bonferroni's post hoc correction. *, $P < 0.05$; **, $P < 0.01$; ***, $P < 0.001$.

were prominent on both days 14 and 21 (Fig. 4 C). Being GC derived, these affinity-matured MBCs were $BrdU^-$. $CD38^{hi}$ MBCs that retained BrdU were also present on days 14 and 21 and, as would be expected for GC-independent MBCs, retained low affinity for HEL^{3X} (Fig. 4 C). Analysis of these distinct GC-independent and GC-dependent MBC populations revealed that they comprised predominantly of $CD80^-$, IgM^+ and $CD80^+$, IgG^+ MBCs, respectively (Fig. 4 C), as would be predicted from

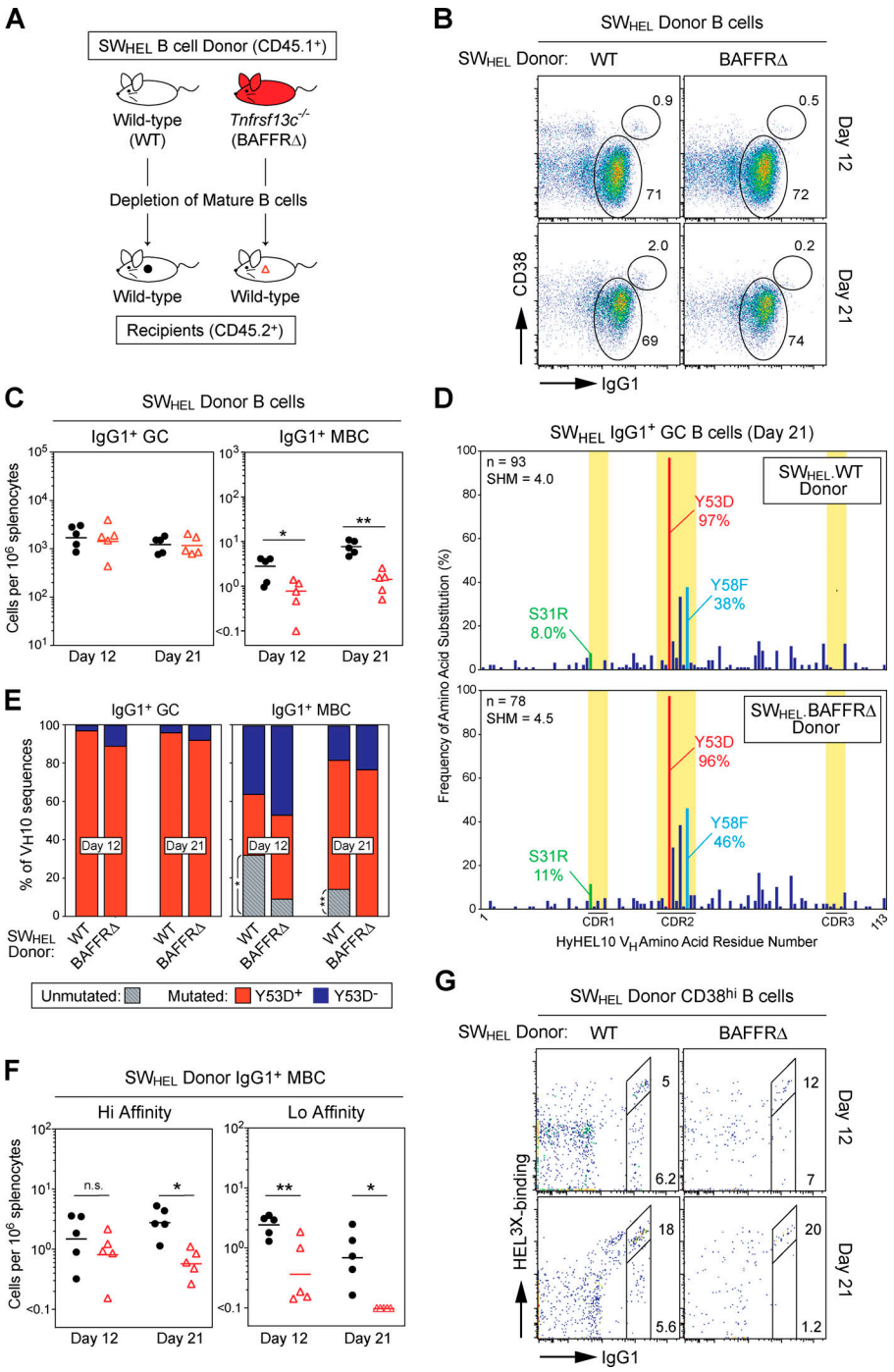

Figure 3. **GC responses progress normally but GC-independent MBC responses are impaired in the absence of BAFFR expression.** **(A)** Transfer strategy to examine immature WT and BAFFRΔ B cell responses. SW_{HEL}.WT or SW_{HEL}.BAFFRΔ splenocytes were MACS enriched for immature B cells ($CD23^{lo}$, $CD21/35^{lo}$, $CD93^{hi}$). Immature WT or BAFFRΔ SW_{HEL} splenocytes were adoptively transferred into WT recipient mice and challenged with HEL^{3X}-SRBC. Recipient mice of WT (black dots) or BAFFRΔ (red triangles) donor cells were antigen boosted on day 4 and harvested on days 12 and 21. **(B)** Flow cytometric analysis of donor-derived WT or BAFFRΔ SW_{HEL} B cells ($CD45.1^+$, $CD45.2^-$, $B220^+$), with gates showing $IgG1^+$ GC B cells ($IgG1^+$, $CD38^{lo}$) and $IgG1^+$ MBCs ($IgG1^+$, $CD38^{hi}$) in WT recipient mice on day 12 (top) and day 21 (bottom). **(C)** Enumeration of WT and BAFFRΔ SW_{HEL} $IgG1^+$ GC B cells (left) and $IgG1^+$ MBCs (right) in WT recipients on days 12 and 21. **(D)** SHM analysis of day 21 single-cell–sorted WT (top) or BAFFRΔ (bottom) SW_{HEL} $IgG1^+$ GC B cells in WT recipients. Skyscraper plot shows the percentage of mutation at each amino acid residue of SW_{HEL} B cell (HyHEL10) heavy chain variable region V_H10. CDR1, CDR2, and CDR3 are highlighted in yellow. High-affinity mutations to HEL^{3X}: Y53D in red; additional affinity-increasing mutations: Y58F in blue and S31R in green. n = number of clones analyzed; SHM = average number of mutations per clone. SHM data represent five pooled recipient mice from one experiment and are representative of two independent experiments. **(E)** Proportion of WT and BAFFΔ SW_{HEL} $IgG1^+$ GC (left) and $IgG1^+$ MBC (right) clones on days 12 and 21: with no mutation (gray), with high-affinity Y53D mutation (red), or with low-affinity without Y53D mutation (blue) in V_H10 obtained from single-cell SHM analysis. SHM data in D and E represent five pooled recipient mice from one experiment and are representative of two independent experiments. Numbers of clones analyzed (n, from left to right) = 58, 75, 73, 79, 31, 45, 28, 22. SHM data were analyzed using χ^2 test (CI = 99%); significance in frequency of unmutated clones is denoted by the following P values: *, $P < 0.05$; **, $P < 0.01$. **(F)** Enumeration of WT and BAFFRΔ HEL^{3X}-binding high-affinity (left) and low-affinity (right) SW_{HEL} $IgG1^+$ MBCs in WT recipient mice on day 14. Enumerated data in C and F were analyzed using an unpaired Student's *t* test with Welch's post hoc correction; *, $P < 0.05$; **, $P < 0.01$; or n.s. (not significant). **(G)** Flow cytometric analysis of WT or BAFFRΔ SW_{HEL} $CD38^{hi}$ B cells ($B220^{hi}$, $CD38^{hi}$) with gates showing $IgG1^+$ HEL^{3X}-binding high- and low-affinity MBC compartments in WT recipients on days 12 and 21. Flow data in B and G represent five concatenated mice from one experiment and are representative of two independent experiments.

previous analyses of mouse MBC subsets (Anderson et al., 2007; Zuccarino-Catania et al., 2014).

To test the impact of BAFF depletion on these two MBC populations, BAFF-neutralizing or isotype control mAbs were administered on day 2 after HEL^{3X}-SRBC challenge, and responding SW_{HEL} B cells were analyzed on days 4 and 14 (Fig. 4 D). Effective neutralization of BAFF was evident from the approximately threefold decrease in total B cell numbers in mice treated with anti-BAFF for 12 d (day 14 of the response; Fig. S4 A). Because anti-BAFF treatment did not affect the number of $B220^-$ non–B cells in the spleen, the size of the various B cell subsets could be expressed relative to this internal control population to avoid introducing additional variability through manual counts of total spleen cell numbers. This analysis revealed that depletion of B cells had already occurred by day 4 of the response, 2 d after the initiation of anti-BAFF treatment

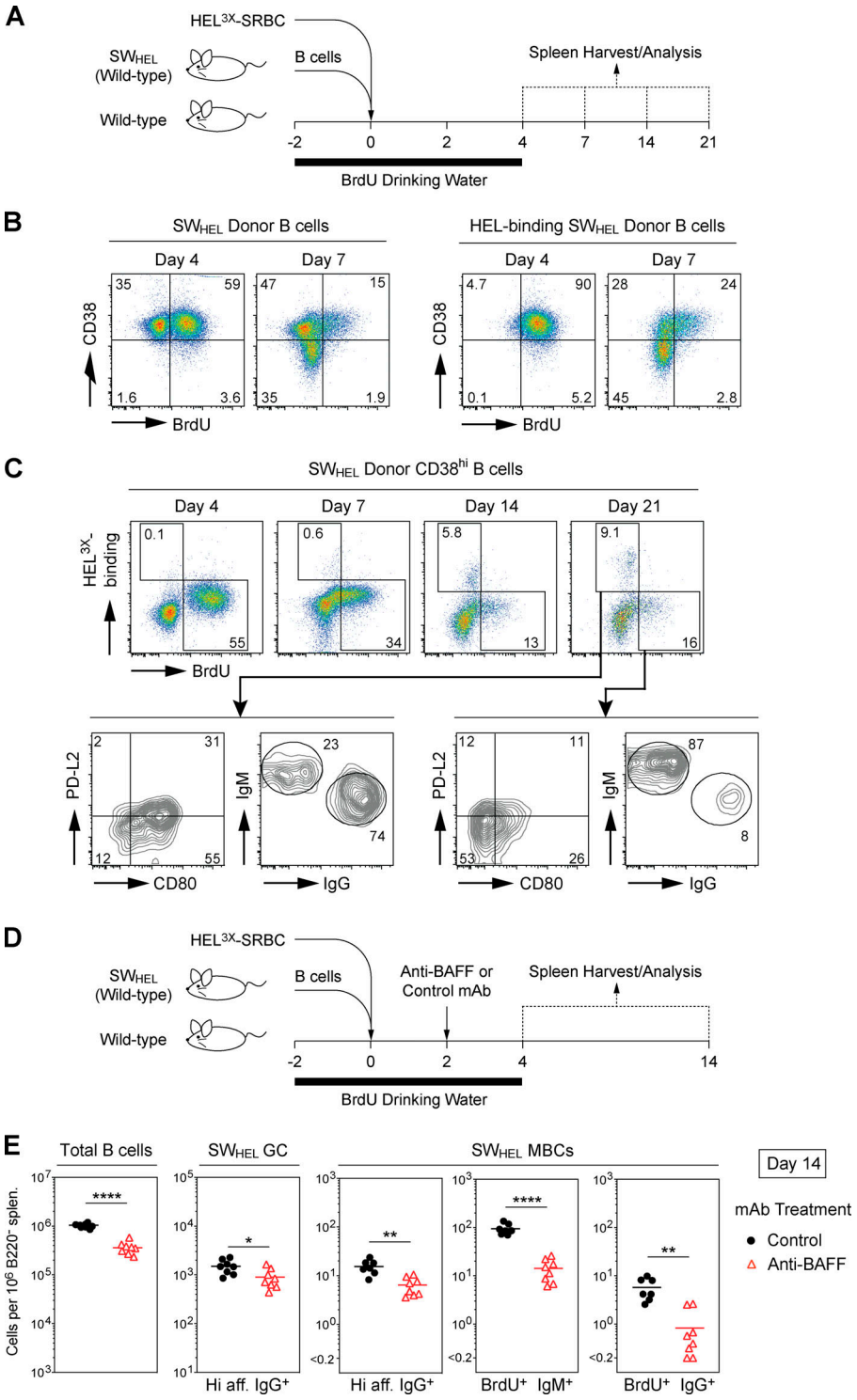

Figure 4. **Acute BAFF depletion preferentially impairs the GC-independent MBC response. (A)** Transfer strategy to track GC-independent and GC-derived MBCs in WT B cell responses. WT recipient mice were placed on BrdU drinking water 2 d before receiving SW_{HEL} donor cells (day −2). WT SW_{HEL} B cells ($CD45.1^+$) were adoptively transferred and challenged with HEL^{3X}-SRBC (day 0). Recipient mice were either harvested on day 4 for analysis or replaced with normal water to be analyzed on days 7, 14, and 21. **(B)** Flow cytometric analysis of donor-derived ($CD45.1^+$, $CD45.2^-$) total SW_{HEL} B cells ($B220^+$; left) and HEL-binding SW_{HEL} B cells ($B220^+$, HEL-binding$^+$; right). Quadrant gates showing the following (clockwise from top left): unlabeled naive or activated B cell ($BrdU^-$, $CD38^{hi}$), BrdU-labeled activated blast and MBC ($BrdU^+$, CD38hi), BrdU-labeled GC B cell ($BrdU^+$, $CD38^{lo}$), and unlabeled GC B cell ($BrdU^-$, $CD38^{lo}$) compartments on days 4 and 7 in WT recipients. **(C)** Flow cytometric analysis of SW_{HEL} $CD38^{hi}$ B cells ($B220^{hi}$, $CD38^{hi}$) with gates showing BrdU-labeled HEL^{3X}-binding low-affinity ($BrdU^+$, HEL^{3Xlo}) and unlabeled high-affinity ($BrdU^-$, HEL^{3Xlo}) MBC compartments in WT recipients on days 4, 7, 14, and 21. $BrdU^+$ low-affinity and $BrdU^-$ high-affinity MBC populations were further analyzed on day 21 for surface CD80 versus PD-L2 expression and categorized into unswitched (IgM^+) or isotype-switched (IgG^+) MBCs. Flow data in B and C represent four concatenated mice from one experiment and are representative of two independent experiments. **(D)** Transfer and treatment strategy to examine BAFF neutralization on WT B cell responses. WT recipient mice were placed on BrdU drinking water and immunized with SW_{HEL} B cells and HEL^{3X}-SRBC on day 0 as described in A, except that recipients were treated with either mouse IgG1κ isotype control or anti-BAFF blocking antibody on day 2. Recipients were either harvested on day 4 for analysis or replaced with normal water for analysis on day 14. **(E)** Enumeration of B cell responses in mice treated with isotype control (black dots) or anti-BAFF (red triangles) antibody. From left to right: Total splenic B cells ($CD45.1^+$, $CD45.2^+$, $B220^+$), donor-derived ($CD45.1^+$, $CD45.2^-$) SW_{HEL} IgG^+ high-affinity GC B cells ($IgG1^+$, $CD38^{lo}$, HEL^{3Xhi}), SW_{HEL} IgG^+ high-affinity MBCs ($IgG1^+$, $CD38^{hi}$, HEL^{3Xhi}), SW_{HEL} GC-independent unswitched MBCs ($BrdU^+$, IgM^+, $CD38^{hi}$), and SW_{HEL} GC-independent IgG-switched MBCs ($BrdU^+$, IgG^+, $CD38^{hi}$). Enumerated data represent eight recipient mice from one experiment and are representative of three independent experiments. Enumerated data were analyzed using an unpaired Student's *t* test with Welch's post hoc correction; *, $P < 0.05$; **, $P < 0.01$; ****, $P < 0.0001$.

(Fig. S4 A). Nevertheless, BAFF depletion had no impact on the early (day 4) response of donor SW_{HEL} B cells (Fig. S4, B and C). By day 14, analysis of GC B cell responses revealed that treatment with anti-BAFF had no significant impact on IgG class switching or positive selection of cells with high affinity for HEL^{3X} (Fig. S4 D). However, it did result in a small decrease in the number of total and high-affinity IgG^+ GC B cells present by day 14 of the response (Fig. 4 E and Fig. S4 C).

In contrast to the GC response, BAFF depletion had a major impact on the numbers of donor-derived, CD38^{hi} B cells present on day 14, reducing the frequency of this population by greater than fivefold (Fig. S4 C). Breakdown of this population into the various MBC subsets (using the gates depicted in Fig. 4 C) revealed that the frequency of both IgM$^+$ and IgG$^+$ GC-independent MBCs (CD38^{hi}, BrdU$^+$) had decreased by 7.2-fold and 8.6-fold, respectively, in anti-BAFF–treated recipients, significantly ($P < 0.001$) more than the 2.5-fold decrease in the numbers of affinity-matured, IgG$^+$ post-GC MBCs that accompanied the reduced GC response (Fig. 4 E). Thus, like B cell–intrinsic BAFFR expression, availability of BAFF is required to obtain an optimal GC-independent MBC response but not the production of GC-dependent MBCs.

Established GC-dependent and GC-independent MBCs can be BAFF dependent

The data obtained thus far pointed strongly to a requirement for cell-intrinsic BAFF/BAFFR signaling in the formation of the GC-independent, but not the GC-dependent, MBC pool. However, despite the normal generation of GC-dependent MBCs by BAFFR-deficient SW$_{HEL}$ B cells on day 12, we did observe a reduction in the number of these affinity-matured cells at a later time point (day 21; Fig. 3, F and G), suggesting that BAFFR may be involved in sustaining the longer-term survival of these cells. To clarify the role of BAFF/BAFFR signaling in long-term MBC survival in our system, we once again labeled GC-independent MBCs via BrdU administration during the early phase of the SW$_{HEL}$.WT B cell response to HEL^{3X}-SRBC, but this time we delayed administration of BAFF-neutralizing mAb until a point (day 21) when stable GC-dependent and GC-independent MBC populations had been established (Fig. 5, A and B). Surprisingly, neutralization of BAFF for 8 d (until day 29) depleted both GC-dependent (high-affinity) and GC-independent (BrdU$^+$; low-affinity) MBCs in the spleen to a degree similar to that in total splenic B cells (Fig. 5 C). As a result, the proportions of these two MBC subpopulations among donor-derived CD38^{hi} B cells were not altered by BAFF blockade (Fig. 5 B), despite the reduction in their overall numbers (Fig. 5 C). BAFF neutralization impacted total B cell numbers in peripheral LNs even more strongly, resulting in an ∼10-fold depletion compared with ∼3-fold in the spleen (Fig. 5 D). Accordingly, depletion of GC-dependent (high-affinity) and GC-independent (BrdU$^+$; low-affinity) MBCs was also more extensive in peripheral LNs (Fig. 5 D). Thus, in this experimental system, there is a clear requirement for BAFF to support the longer-term survival of both GC-dependent and GC-independent MBCs as well as naive B cells.

To directly test the impact of BAFF depletion on MBC-dependent secondary responses, a separate cohort of mice that had undergone primary challenge and treatment with either control or anti-BAFF mAb were supplemented with naive OT-II TCR transgenic CD4$^+$ T cells (day 28) and 24 h later were challenged s.c. with HEL conjugated to the I-A^b restricted OVA peptide recognized by OT-II (HEL-OVA; Fig. 5 A). After 6 d, the numbers of donor-derived SW$_{HEL}$ B cells in draining LNs increased by 5–10-fold, regardless of prior BAFF depletion (Fig. 5, E and F; and Fig. S4 E). Recall responses at this point comprised mostly GC B cells as well as smaller population of PCs. The magnitude of the recall responses on day 35 in each case reflected the size of the day 29 MBC pool, therefore being ∼10-fold lower in mice that had undergone BAFF depletion (Fig. 5, E and F; and Fig. S4, E and F). Recall responses contained both IgG$^+$ switched and IgM$^+$ unswitched GC B cells and PCs (Fig. 5, G and H; and Fig. S5 B). GC responses were made up predominantly of cells with low affinity for the HEL^{3X} primary antigen (Fig. 5, G and H), whereas the cells with high affinity for HEL^{3X} were more frequent in the PC responses, suggesting that GC-dependent and GC-independent MBCs differentially contributed to these two arms of the secondary response. Overall, however, the major conclusion of this experiment was that neutralization of BAFF in this system depleted both types of long-lived MBCs and impacted the recall response accordingly.

Augmenting BAFFR signaling specifically expands GC-independent MBC responses

Because signaling by BAFF through BAFFR on responding B cells is specifically required to obtain the GC-independent MBC response, we reasoned that this component of T-dependent B cell responses may be selectively augmented by increasing the magnitude of this signal. To test this, we first used a retroviral transduction approach to overexpress BAFFR on responding SW$_{HEL}$ B cells and examined the impact on their response to antigen in WT recipients (Fig. 6 A). In vitro transduction of SW$_{HEL}$ B cells with plasmid murine stem cell virus (pMSCV)–based retroviral vectors carrying an internal ribosome entry site (IRES)–GFP reporter was followed by transfer and challenge with HEL^{3X}-SRBC and analysis of donor-derived responses on days 12 and 21. Transduced (GFP$^+$) donor cells carrying the BAFFR-encoding vector were verified to overexpress surface BAFFR by flow cytometry (Fig. S5 A). Although BAFFR overexpression had a small, transient impact on the size of the GC response (Fig. 6 B), there was no effect on either IgG1 class switching (Fig. 6 C) or SHM and selection for high-affinity HEL^{3X}-binding GC B cells (Fig. 6, C and D). However, BAFFR overexpression led to increased numbers of CD38^{hi} IgG1-switched MBCs (Fig. 6 B and Fig. S5 B) due to a selective increase in the numbers of low-affinity (Fig. 6, E and F) and unmutated (Fig. 6 G) MBCs, indicating that it had caused a specific expansion of the GC-independent MBC response.

We have previously shown that the TRAF3 signaling adapter acts as a potent negative regulator of BAFFR signaling in B cells (Gardam et al., 2008). We therefore also asked whether SW$_{HEL}$ B cells that lacked TRAF3 expression (SW$_{HEL}$.TRAF3ΔB) would also produce an expanded GC-independent MBC response (Fig. 7 A). TRAF3 inactivation in donor B cells was found to have no detectable effect on their GC responses in terms of size, IgG1 class switching (Fig. 7, B and C), or selection for high-affinity HEL^{3X}-binding B cells (Fig. 7, D and E). In contrast, SW$_{HEL}$ B cells lacking TRAF3 made an expanded CD38^{hi} IgG1-switched MBC response (Fig. 7, B and C) due exclusively to an increase in the numbers of MBCs with low affinity for HEL^{3X} (Fig. 7, F and G), once again consistent with the selective expansion of the GC-independent MBC response.

Examination of a later time point (day 40) in response to HEL^{2X}-SRBCs indicated that low-affinity MBCs remained greatly

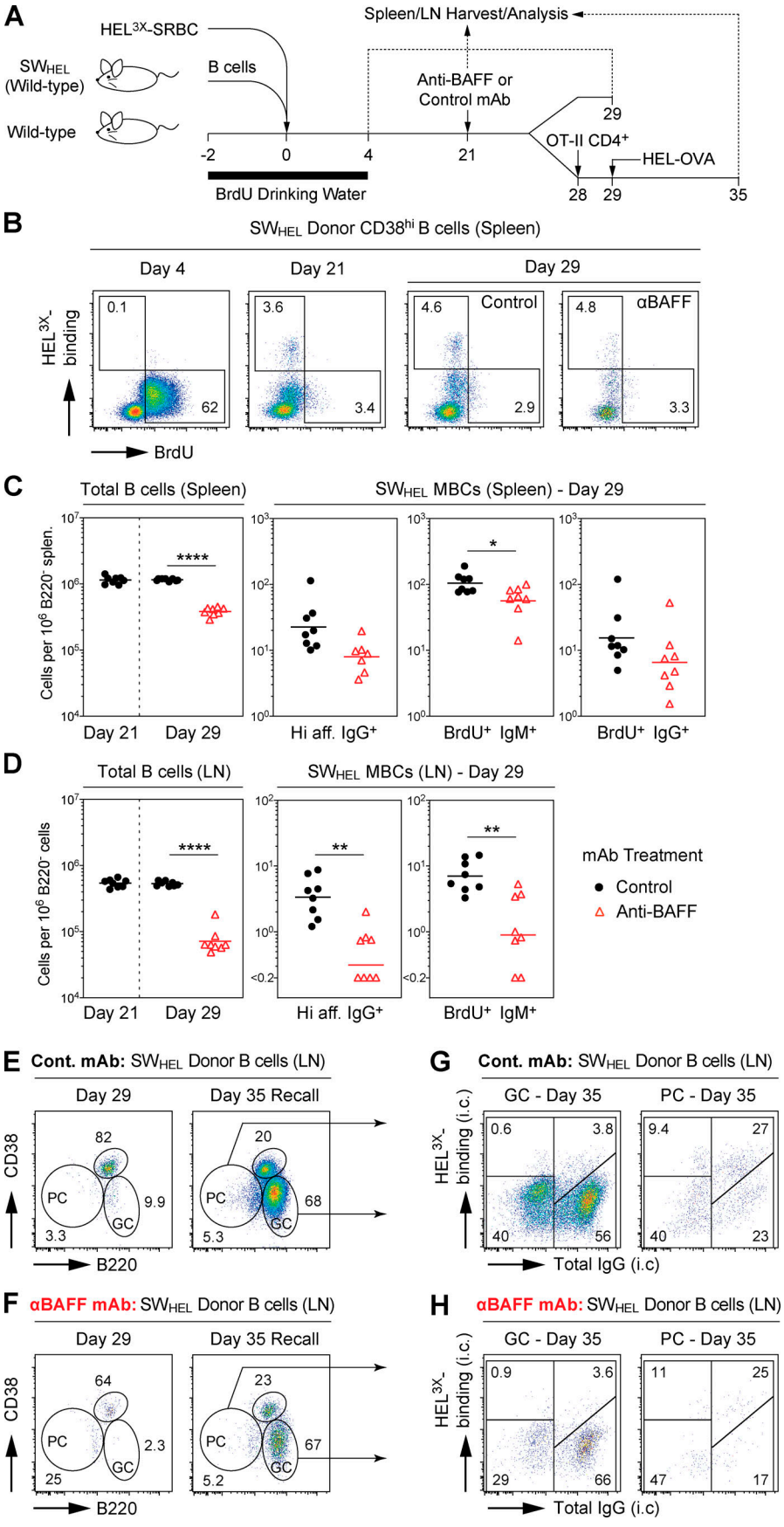

Figure 5. **Established GC-dependent and GC-independent MBCs can be BAFF dependent.** **(A)** Transfer and treatment strategy to examine BAFF neutralization on WT MBC responses. WT recipient mice were placed on BrdU drinking water 2 d before receiving SW_{HEL} donor cells (day −2). WT SW_{HEL} B cells ($CD45.1^+$) were adoptively transferred and challenged with HEL^{3X}-SRBC i.v. (day 0). Recipients were either killed on days 4 and 21 for spleen and LN analysis or placed on normal water from day 4. Mice either were treated with mouse IgG1κ isotype control or anti-BAFF blocking antibody on day 21 or day 29 or received OT-II $CD4^+$ T cells i.v. on day 28 and rechallenged with HEL-OVA s.c. 24 h later (day 29) for analysis of the day 5 recall response (day 35). **(B)** Flow cytometric analysis of donor-derived ($CD45.1^+$, $CD45.2^-$) SW_{HEL} $CD38^{hi}$ B cells ($B220^{hi}$, $CD38^{hi}$), with gates showing BrdU-labeled HEL^{3X}-binding low-affinity ($BrdU^+$, HEL^{3Xhi}) and unlabeled high-affinity ($BrdU^-$, HEL^{3Xlo}) MBC compartments in WT recipients before mAb treatment (days 4 and 21) and 8 d after control or anti-BAFF mAb treatment (day 29). Flow data represent eight concatenated mice from one experiment and are representative of two independent experiments. **(C)** Enumeration of splenic B cell responses in mice treated with isotype control (black dots) or anti-BAFF antibody (red triangles). From left to right: Total splenic B cells ($CD45.1^+$, $CD45.2^+$, $B220^+$) before (day 21) and after (day 29) treatment, donor-derived ($CD45.1^+$, $CD45.2^-$) SW_{HEL} IgG^+ high-affinity MBCs ($IgG1^+$, $CD38^{hi}$, HEL^{3Xhi}), SW_{HEL} GC-independent unswitched MBCs ($BrdU^+$, IgM^+, $CD38^{hi}$), and SW_{HEL} GC-independent IgG-switched MBCs ($BrdU^+$, IgG^+, $CD38^{hi}$) on day 29. **(D)** Enumeration of LN B cell responses in mice treated with isotype control (black dots) or anti-BAFF (red triangles) antibody. From left to right: Total B cells in inguinal LNs before (day 21) and after (day 29) treatment, SW_{HEL} IgG^+ high-affinity MBCs, and SW_{HEL} GC-independent unswitched MBCs on day 29. Enumerated data in C and D represent eight replicate mice from one experiment and are representative of two independent experiments. Enumerated data were analyzed using an unpaired Student's *t* test with Welch's post hoc correction; *, $P < 0.05$; **, $P < 0.01$; ****, $P < 0.0001$. **(E)** Flow cytometric analysis of SW_{HEL} B cell responses in paired inguinal LNs of isotype control–treated recipients and **(F)** anti-BAFF mAb–treated recipients before HEL-OVA challenge (day 29) and 5 d after rechallenge (day 35), with gates showing GC B cells ($B220^{hi}$, $CD38^{lo}$), $CD38^{hi}$ B cells ($B220^{hi}$, $CD38^{hi}$), and PCs ($B220^{lo}$, $CD38^{int}$). **(G)** Flow cytometric analysis of day 5 recall SW_{HEL} GC and PC responses (arrows from E) of control mAb-treated mice, with gates showing intracellular (i.c.) IgG versus HEL^{3X}-binding high- and low-affinity compartments. **(H)** Flow cytometric analysis of day 5 recall SW_{HEL} GC and PC responses (arrows from F) of anti-BAFF mAb–treated mice, with gates showing IgG (i.c.) versus HEL^{3X}-binding (i.c.) high- and low-affinity compartments. Flow data in E–H represent five concatenated mice from one experiment and are representative of two independent experiments.

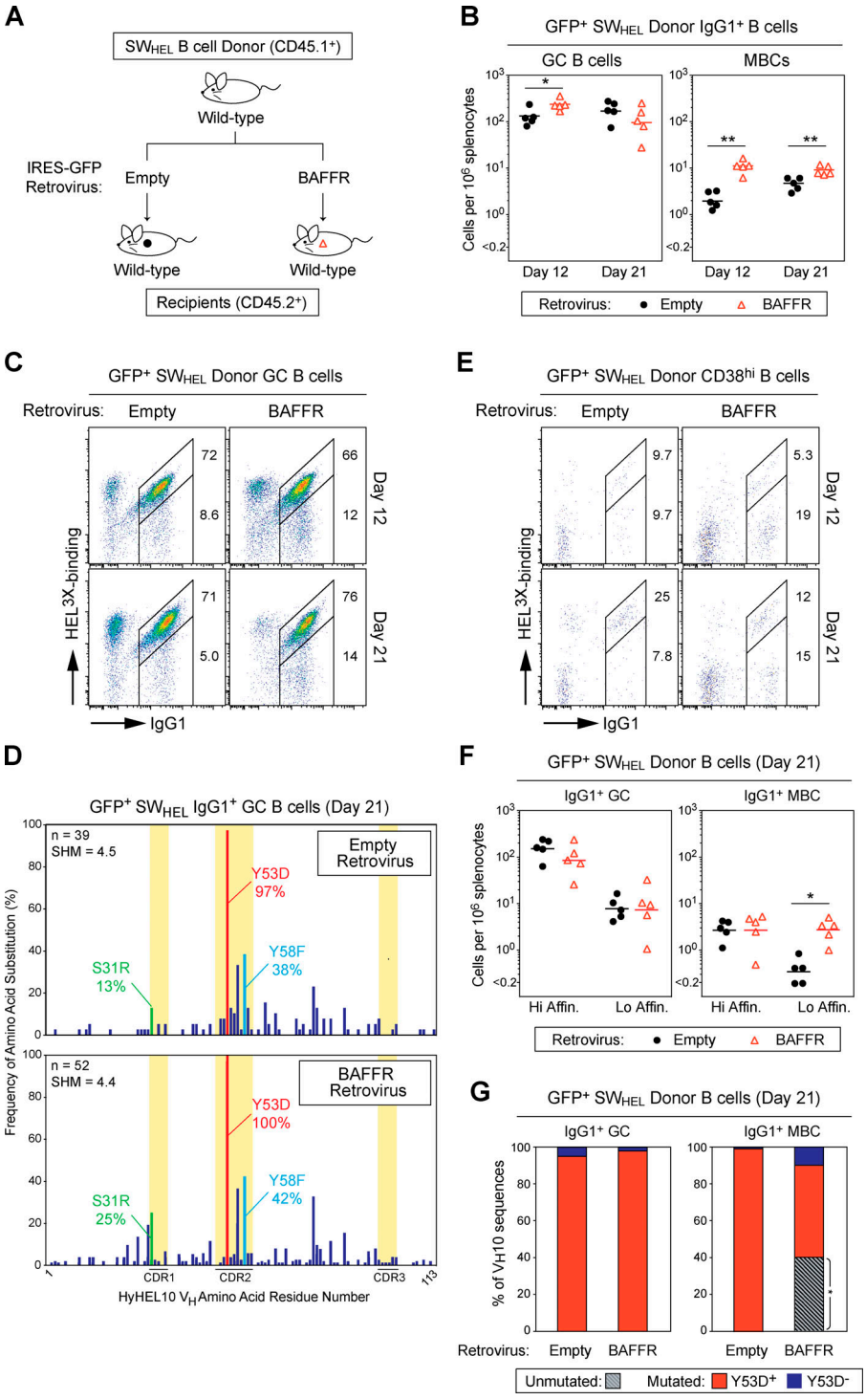

Figure 6. **Increased BAFFR expression specifically expands GC-independent MBC responses. (A)** Transfer strategy to examine the impact of BAFFR overexpression on T-dependent B cell responses. SW_{HEL} B cells were stimulated in vitro and transduced with retrovirus (RV) containing overexpression GFP vector encoding BAFFR protein under the control of 5′-LTR–mediated transcription. RV-containing empty GFP vector was used as a control (Empty). RV-transduced SW_{HEL} B cells (GFP^+, $CD45.1^+$) were adoptively transferred into WT ($CD45.2^+$) recipient mice and challenged with HEL^{3X}-SRBC. Recipients of Empty (black dots) or BAFFR (red triangles) transduced donor cells were antigen boosted on day 4 and analyzed on days 12 and 21. IRES, internal ribosome entry site. **(B)** Enumeration of donor-derived ($CD45.1^+$, $CD45.2^-$, $B220^+$) transduced SW_{HEL} $IgG1^+$ GC B cells (GFP^+, $IgG1^+$, $CD38^{lo}$; left) and transduced $IgG1^+$ MBCs (GFP^+, $IgG1^+$, $CD38^{hi}$; right) in WT recipients on days 12 and 21. **(C)** Flow cytometric analysis of Empty or BAFFR-transduced SW_{HEL} GC B cells (GFP^+, $B220^{hi}$, $CD38^{lo}$), with gates showing $IgG1^+$ HEL^{3X}-binding high- and low-affinity GC compartments in WT recipients on day 12 (top) and day 21 (bottom). **(D)** SHM analysis of day 21 single-cell–sorted GFP^+ SW_{HEL} $IgG1^+$ GC B cells from Empty or BAFFR-transduced donor responses. Skyscraper plot shows the percentage of mutation at each amino acid residue of SW_{HEL} B cell (HyHEL10) heavy chain variable region V_H10. CDR1, CDR2, and CDR3 are highlighted in yellow. High-affinity mutations to HEL^{3X}: Y53D in red; additional affinity-increasing mutations: Y58F in blue and S31R in green. n = number of clones analyzed; SHM = average number of mutations per clone. **(E)** Flow cytometric analysis of Empty or BAFFR-transduced SW_{HEL} $CD38^{hi}$ B cells (GFP^+, $B220^{hi}$, $CD38^{hi}$), with gates showing $IgG1^+$ HEL^{3X}-binding high- and low-affinity MBC compartments in WT recipients on day 12 (top) and day 21 (bottom). Flow data in C and E represent five concatenated mice from one experiment and are representative of three independent experiments. **(F)** Enumeration of GFP^+ HEL^{3X}-binding high- and low-affinity $IgG1^+$ GC B cells (left) and $IgG1^+$ MBCs (right) in empty (black dots) or BAFFR-transduced (red triangles) SW_{HEL} donor responses in WT recipients on day 21. Enumerated data in B and F were analyzed using an unpaired Student's *t* test with Welch's post hoc correction; *, $P < 0.05$; **, $P < 0.01$. **(G)** SHM analysis of day 21 single-cell–sorted Empty or BAFFR-transduced SW_{HEL} GFP^+ $IgG1^+$ GC and GFP^+ $IgG1^+$ MBC clones in WT recipients. Proportion of $IgG1^+$ GC (left) and $IgG1^+$ MBC (right) clones with no mutation (gray), with high-affinity Y53D mutation (red), or with low-affinity without Y53D mutation (blue) in SW_{HEL} B cell (HyHEL10) heavy chain variable region V_H10. Numbers of clones analyzed (n, from left to right) = 39, 52, 14, 11. SHM data were analyzed using the χ^2 test (CI = 99%); significance in frequency of unmutated clones is denoted by P value: *, $P < 0.05$. SHM data in D and G represent five pooled recipient mice from one experiment and are representative of three independent experiments.

expanded in responses mounted by TRAF3-deficient SW_{HEL} B cells (Fig. S5, C and D). SHM analysis revealed that this correlated with a 10-fold higher frequency of unmutated clones among donor-derived B cells (Fig. S5 E), confirming that removal of TRAF3 expression from responding B cells had greatly expanded the GC-independent MBC compartment. Unlike earlier time points, the number of high-affinity GC-dependent MBCs was also increased on day 40 of the SW_{HEL}.TRAF3ΔB B cell response (Fig. S5 E), presumably reflecting the role of BAFFR signaling in promoting the longer-term survival of these

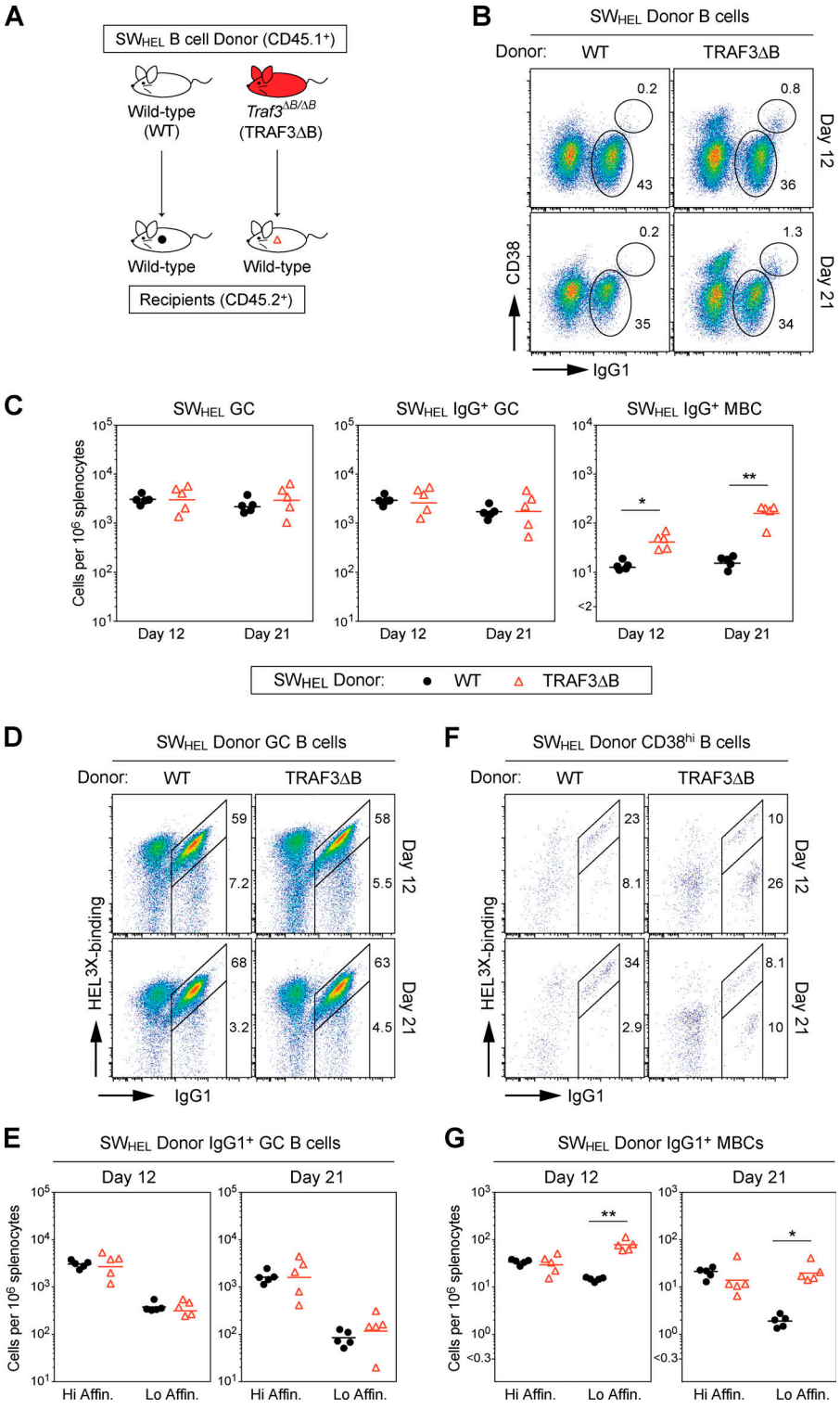

Figure 7. **Removal of TRAF3 expression specifically expands GC-independent MBC responses. (A)** Transfer strategy to examine the impact of cell-intrinsic hyperactivated BAFFR signaling by TRAF3 inactivation on T-dependent B cell responses. SW_{HEL} mice were crossed onto *Traf3*$^{\Delta B/\Delta B}$ mice to generate SW_{HEL} mice with B cell–restricted TRAF3 inactivation (SW_{HEL}.TRAF3ΔB). WT or TRAF3ΔB SW_{HEL} splenocytes (CD45.1$^+$) were adoptively transferred into WT (CD45.2$^+$) recipient mice and challenged with HEL^{3X}-SRBC. Recipient mice of WT (black dots) or TRAF3ΔB (red triangles) donor cells were antigen boosted on day 4 and harvested on days 12 and 21. **(B)** Flow cytometric analysis of donor-derived WT or TRAF3ΔB SW_{HEL} B cells (CD45.1$^+$, CD45.2$^-$, B220$^+$), with gates showing IgG1$^+$ GC B cells (IgG1$^+$, CD38^{lo}) and IgG1$^+$ MBC (IgG1$^+$, CD38^{hi}) in WT recipients on day 12 (top) and day 21 (bottom). **(C)** Enumeration of WT or TRAF3ΔB SW_{HEL} GC B cells (B220^{hi}, CD38^{lo}; left), IgG1$^+$ GC B cells (IgG1$^+$, CD38^{lo}; center), and IgG1$^+$ MBCs (IgG1$^+$, CD38^{hi}; right) in WT recipients on days 12 and 21. **(D)** Flow cytometric analysis of WT or TRAF3ΔB SW_{HEL} GC B cells (B220^{hi}, CD38^{lo}), with gates showing IgG1$^+$ HEL^{3X}-binding high- and low-affinity GC compartments in WT recipients on day 12 (top) and day 21 (bottom). **(E)** Enumeration of HEL^{3X}-binding high- and low-affinity compartments in WT or TRAF3ΔB SW_{HEL} IgG1$^+$ GC B cells on day 12 (left) and day 21 (right). **(F)** Flow cytometric analysis of WT or TRAF3ΔB SW_{HEL} CD38^{hi} B cells (B220^{hi}, CD38^{hi}), with gates showing IgG1$^+$ HEL^{3X}-binding high- and low-affinity MBC compartments in WT recipients on day 12 (top) and day 21 (bottom). Flow data represent five replicate mice from one experiment and are representative of three independent experiments. Flow data in B, D, and F represent five mice from one experiment and are representative of three independent experiments. **(G)** Enumeration of HEL^{3X}-binding high- and low-affinity compartments in WT or TRAF3ΔB SW_{HEL} IgG1$^+$ MBCs on day 12 (left) and day 21 (right). Enumerated data in C, E, and G were analyzed using an unpaired Student's *t* test with Welch's post hoc correction; *, $P < 0.05$; **, $P < 0.01$.

cells in this system (Fig. 5, C and D). Recall responses initiated with HEL^{2X}-HRBCs i.v. on day 40 and analyzed 5 d later revealed that unmutated, GC-independent MBCs disproportionately contributed to the secondary responses mounted by both WT and TRAF3-deficient B cells (Fig. S5 E), consistent with the results obtained earlier in HEL-OVA recall responses (Fig. 5, G and H). Taken together, these results establish GC-independent MBCs as an important contributor to secondary T-dependent B cell responses and confirm that the formation of this MBC pool is specifically and potently increased by the augmentation of BAFFR signaling in responding B cells.

Discussion

The identification of BAFF and BAFFR and their key role in supporting the survival of mature, naive B cells fundamentally

changed our understanding of B cell homeostasis (Mackay et al., 2003). However, the depletion of mature B cells and compromised development of stromal cells that occur in the absence of BAFF or BAFFR have made it difficult to assess their roles in B cells participating in downstream immune responses. By circumventing these problems using several complementary approaches, we have shown that BAFFR signaling in B cells is dispensable in the GC response and for the production of MBCs that derive from GC B cell precursors. However, BAFF-mediated triggering of BAFFR expressed on responding B cells was found to be essential for the development of the population of unswitched (IgM^+) and class-switched (IgG^+) MBCs that arise early in the response independent of the GC reaction.

Although GCs are transient in the global absence of BAFF or BAFFR, previous studies have shown that SHM still occurs among GC B cells under these circumstances (Rahman et al., 2003; Vora et al., 2003). Our data confirmed not only that BAFFR signaling in GC B cells is not required for SHM but also that it is dispensable for their survival and affinity maturation, as well as their differentiation into MBCs and the production of high-affinity antibodies. A previous study has indicated that BAFF provided by Tfh cells can play a role in GC B cell affinity maturation (Goenka et al., 2014). However, consistent with the absence of any obvious function for BAFFR in GC B cells, we did not detect a significant role for Tfh cell–derived BAFF in regulating the GC response in our experimental system. Possible explanations for this discrepancy between the two studies include differences in the target epitope (chemical hapten versus conformational protein epitope), the carrier responsible for recruiting $CD4^+$ T cell help (OVA versus SRBC), and the presence versus absence of alum adjuvant (Goenka et al., 2014). It remains possible that the kinetics of selection of high-affinity GC B cells was slower in our system in the absence of Tfh cell–derived BAFF but not detected by our analysis. However, we did not see an effect on the accumulation of high-affinity GC B cells early in the response (day 14), so any impact would have been a relatively subtle one. We did observe a small (but not statistically significant) reduction in the levels of high-affinity serum IgG1 when Tfh cells could not produce BAFF. Because Goenka et al. (2014) observed a greater impact upon affinity maturation of serum antibody as opposed to GC B cell selection per se, it may be that the major impact of Tfh cell–derived BAFF is upon GC-derived PCs and that it acts via either the transmembrane activator and calcium-modulating ligand interactor (TACI) receptor or the B cell maturation antigen (BCMA) receptor rather than BAFFR.

The data described here demonstrate that the production of GC-independent MBCs during the early phase of a primary T-dependent B cell response is exquisitely sensitive to B cell–intrinsic signals delivered through the BAFF/BAFFR signaling pathway. This was evident through the specific depletion of these cells early in the response when either BAFFR expression or BAFF availability was removed but also by the selective expansion of this MBC population when BAFFR signals were augmented by either BAFFR overexpression or removal of TRAF3 expression. Although TRAF3 has multiple functions that could potentially influence B cell responses, the fact that TRAF3 inactivation and BAFFR overexpression in responding B cells had identical impacts on the GC-independent MBC response strongly suggests that removal of negative regulation of BAFFR signaling was the mechanism underlying the phenotype associated with TRAF3 deficiency (Gardam et al., 2008).

In contrast to the specific requirement for BAFF/BAFFR signaling in the formation of GC-independent but not GC-dependent MBC responses, we obtained the somewhat unexpected result that this signaling pathway plays a role in the long-term survival of both these MBC populations in our experimental system. This result contrasted with results of earlier studies in mice showing that depletion of BAFF did not have a significant impact on MBC numbers (Benson et al., 2008; Scholz et al., 2008). The role of BAFF/BAFFR signaling in the survival of MBCs in our study was apparent not only from the depletion of both MBC subsets together with naive B cells upon BAFF neutralization but also by the fact that the numbers of high-affinity, GC-dependent MBCs declined when they did not express BAFFR and increased when they lacked TRAF3 expression. It appears, therefore, that the survival of established MBCs is not always independent of BAFF/BAFFR signaling. Because our experiments focused on MBCs generated relatively early in a primary response (up to 4 wk), it is possible that MBCs that persist in the longer term are less dependent on the survival signals delivered through the BAFF/BAFFR pathway. Indeed, the two previous studies in mice examined MBCs at either 18–26 wk (Benson et al., 2008) or 8–12 wk (Scholz et al., 2008) that had been established from a primary immunization. Alternatively, in contrast to our present study, both of these earlier investigations used protein antigens in alum adjuvant, which could conceivably alter the survival characteristics of long-term MBCs. Interestingly, treatment of systemic lupus erythematosus patients with the BAFF-neutralizing mAb belimumab has been reported to have a range of impacts upon peripheral blood MBCs, including a temporary increase followed by a decrease in the numbers of class-switched MBCs (Stohl et al., 2012), no effect on the class-switched MBC population (Jacobi et al., 2010), and a decrease in the numbers of unswitched (Jacobi et al., 2010) or "double-negative" (Ramsköld et al., 2019) MBCs. Recall responses to antigens present in the seasonal influenza vaccine were also shown to be reduced in patients treated with belimumab (Chatham et al., 2012), whereas rare patients with a specific genetic deficiency in BAFFR expression displayed variable impacts on MBC numbers and responses to vaccination (Warnatz et al., 2009). In light of these data and the results reported here, it appears that the role of BAFF/BAFFR signaling in sustaining long-term MBC survival may vary according to a set of parameters that are yet to be defined.

It has been speculated that the formation of GC-independent MBCs, in effect an expanded pool of unmutated primary specificities directed against a foreign pathogen, may provide the basis for rapid responses against mutant or related pathogens that may evade the more specific, affinity-matured, GC-dependent MBCs (Takemori et al., 2014; Tarlinton and Good-Jacobson, 2013). Our finding that the development of a GC-independent MBC pool is uniquely dependent on BAFF/BAFFR signaling suggests that there could be some advantage to immune protection in

regulating the survival of these MBCs independently of the GC-dependent MBC response. For example, the presence of excess circulating BAFF that occurs in mice and humans with B lymphopenia (Kreuzaler et al., 2012) may help compensate for the contracted primary repertoire by augmenting the GC-independent MBC compartment, much like the results we observed when B cells overexpressed BAFFR or lacked TRAF3. This same phenomenon presumably explains the dramatic expansion of GC-independent MBCs we observed when WT SW_{HEL} B cells were challenged with HEL^{3X}-SRBCs in BAFFRΔ recipient mice. It seems likely, therefore, that variations in BAFF levels between different individuals or disease states may significantly impact the formation of GC-independent MBC responses.

Materials and methods

Mice and adoptive transfers

SW_{HEL} mice (Phan et al., 2003) were maintained on a CD45.1 congenic ($Ptprc^{a/a}$) C57BL/6J background. BAFF-deficient mice ($Tnfsf13b^{-/-}$ = BAFFΔ; Schiemann et al., 2001), BAFFR-deficient mice ($Tnfrsf13c^{-/-}$ = BAFFRΔ; Sasaki et al., 2004), T cell–deficient mice ($Cd3e^{-/-}$; Malissen et al., 1995), and mice lacking TRAF3 expression in B cells ($Traf3^{fl/fl}$.*Cd19*-cre = TRAF3ΔB; Gardam et al., 2008) were either maintained on a C57BL/6 background or crossed with SW_{HEL} mice on a CD45.1 congenic C57BL/6 background in adoptive transfer experiments. OT-II TCR transgenic mice (Barnden et al., 1998) were maintained on a C57BL/6 Thy1.1 congenic ($Thy1^{a/a}$) background. WT C57BL/6 mice were purchased from Australian BioResources. All mice were bred and maintained in specific-pathogen–free conditions at Australian BioResources and the Garvan Institute of Medical Research Biological Testing Facility. Animal experiments were performed under the approved guidelines of the Garvan Institute of Medical Research/St. Vincent's Hospital Animal Ethics Committee. For adoptive transfer experiments, SW_{HEL} B cells and spleen cells containing 3×10^4 HEL-binding B cells were transferred i.v. into CD45.2 congenic recipient mice. All SW_{HEL} B cell recipients were challenged with 2×10^8 HEL^{3X}-SRBCs (prepared as previously described; Paus et al., 2006) and boosted with HEL^{3X}-SRBCs 4 d later. To deplete mature B cells from WT and BAFFRΔ SW_{HEL} donor spleen cells before adoptive transfer, spleen cell preparations were stained with anti-CD23 mAb (B3B4; BioLegend) and anti-CD35 mAb (8C12; BD Biosciences), and $CD23^+CD21/35^+$ cells were depleted using the Miltenyi magnetic-activated cell sorting (MACS) negative selection kit as per the manufacturer's instructions. For memory recall responses, recipients that had received SW_{HEL} B cells and SRBC-HEL^{3X} 28 d earlier received 2.5×10^5 OT-II $CD4^+$ T cells i.v. followed by s.c. challenge 24 h later (day 29) with 40 µg of HEL-OVA in Sigma Adjuvant System (Sigma) in the lower flank and base of the tail. OT-II $CD4^+$ T cells were enriched via MACS negative depletion as described above using biotinylated anti-B220 (RA3-6B2), CD11b (M1/70), CD11c (HL3), and CD8 (53-6.7) mAb (all from BD Biosciences), with OT-II $CD4^+$ T cells at 70–80% purity as determined by FACS analysis. HEL was conjugated to $OVA_{323–339}$ peptide (CGGISQAVHAAHAEINEAGR; mimotopes; GenScript) using succinimidyl-6-([β-maleimidopropionamido]hexanoate; Thermo Fisher Scientific) to generate HEL-OVA as described previously (Moran et al., 2018).

BM chimeras

$Cd3e^{-/-}$ mice of 8-12 wk old were lethally irradiated (2 × 450 rad) using a X-RAD 320 Biological Irradiator (Precision X-Ray). BM cells from donor mice were aspirated into RPMI supplemented with 10% FCS, 55 mM β-mercaptoethanol, 50 units/ml penicillin, and 50 mg/ml streptomycin. Single-cell suspensions consisting of a 20:80 mixture of BM cells from $Cd3e^{-/-}$ and either WT or $Tnfsf13b^{-/-}$ donor mice were injected i.v. into recipient mice 15 h after irradiation (~10^7 cells per recipient). The resulting chimeras were utilized for adoptive transfer experiments 8 wk after reconstitution.

Antibodies and reagents

The following mAbs against mouse IgG1 (A85-1), IgG2b (RMG2b1), $IgG2a^b$ (5.7), IgG3 (R40-82), IgM^b (AF6-78), CD38 (90), CD45R/B220 (RA3-6B2), CD95/Fas (Jo2), CD35 (8C12), CD11b (M1/70), CD11c (HL3), and CD8 (53-6.7) were purchased from BD Biosciences. Antimouse CD45.1 (A20), CD45.2 (104), CD3e (eBio500A2) were obtained from eBioscience. The mAbs against murine CD93/C1qR (AA4.1), CD21/35 (7E9), and CD23 (B3B4) were obtained from BioLegend, and anti-mouse BAFFR (9B9) was purchased from AdipoGen Life Sciences. Streptavidin (SA)-PE, -BV421, and -BUV395 were purchased from BD Biosciences. Purified antimouse CD16/32 (2.4G2) and HyHEL9 mAbs were sourced from the University of California, San Francisco Hybridoma Core, and the latter was conjugated to Alexa Fluor 647 using the Alexa Fluor 647 Protein Labeling Kit (Invitrogen) according to the manufacturer's instructions. Purified anti-CD38 was conjugated to Pacific Orange Antibody Labeling Kit (Invitrogen) according to the manufacturer's instructions. Staining for BrdU incorporation was performed using the FITC BrdU Flow kit (BD Biosciences) according to the manufacturer's instructions.

Flow cytometry

For analysis of adoptive transferred responses, lymphocytes from spleens or LNs were isolated and prepared for cell surface staining for HEL^{WT} or HEL^{3X} binding and other cell surface markers as described elsewhere (Chan et al., 2012). For phenotypic analysis of splenic B cell subsets, spleen cells were stained for surface markers CD21/35, CD23, and CD93/C1qR (Gardam et al., 2008). For flow cytometric analysis of Ig class-switched SW_{HEL} B cells, surface staining was performed with 200 ng/ml of HEL^{WT} or 50 ng/ml of HEL^{3X} followed by anti-IgG1 or a combination of antibodies against IgG1, IgG2b, $IgG2a^b$ (=IgG2c), and IgG3. Samples were then blocked with 10% normal mouse serum (Jackson ImmunoResearch), and bound HEL^{WT} or HEL^{3X} was revealed with Alexa Fluor 647 conjugated HyHEL9 and other surface marker stained with specific mAbs. For staining of intracellular Ig, cells were fixed with 10% formalin (Sigma-Aldrich) after surface staining for B cell markers. Cell permeabilization and subsequent staining steps were performed in 0.5% saponin/0.1% BSA/PBS (Sigma-Aldrich). Intracellular

staining was performed with 50 ng/ml of HEL^{3X} followed by combination of anti-IgG antibodies. Cells were blocked with 10% normal mouse serum, and bound HEL^{3X} was revealed with Alexa Fluor 647–conjugated HyHEL9 in 5% normal mouse serum and fluorochrome-conjugated streptavidin. Data were acquired on either the LSR II special order research product (BD Biosciences) or the LSR Fortessa (BD Biosciences) and analyzed with FlowJo software (TreeStar). Light scatter gating was performed on all samples to include lymphocytes but exclude doublets, dead cells, and debris.

Single-cell SHM analysis

To sort single SW_{HEL} B cells for SHM analysis of the HyHEL10 heavy chain variable region gene, cell suspensions from recipient spleens were prepared and surface stained as detailed in the section describing flow cytometric analysis. Single-cell sorting was performed on the FACSAria and FACSAria II devices (BD Biosciences). The variable region of the HyHEL10 heavy chain gene was amplified by PCR and sequenced as previously described (Paus et al., 2006). DNA sequences of single SW_{HEL} B cell clones were aligned and verified against the HyHEL10 heavy chain variable region coding sequence to identify somatic mutation events. Mutations resulting in amino acid residue changes were identified after translation and alignment against the HyHEL10 heavy chain variable region sequence.

HEL proteins

Purified HEL^{WT} was purchased from Sigma-Aldrich. Recombinant HEL^{2X} and HEL^{3X} proteins were grown as secreted proteins in yeast (*Pichia pastoris*) and purified from culture supernatants as described previously (Paus et al., 2006).

HEL^{3X}-binding ELISA

ELISA detection of HEL^{3X}-specific serum antibodies was performed as described previously (Phan et al., 2003) using HEL^{3X} protein–coated, 384-well plates (Corning). To quantify serum antibody concentrations, endpoint titers were calculated on the basis of 97.5% confidence levels or greater (Frey et al., 1998).

BrdU labeling and BAFF neutralization

To label pre-GC early B cell blasts, recipient mice were placed on BrdU-containing drinking water (0.8 mg/ml; Sigma-Aldrich) 2 d before adoptive transfer and immunization and maintained on BrdU water for 4 d after antigen challenge. To deplete endogenous BAFF, BAFF-neutralizing anti-BAFF mAb (Sandy-2; AdipoGen Life Sciences) or mouse IgG1κ isotype control (MOPC-31; BD Biosciences) was administered i.v. at 2 mg/kg per recipient either 2 d or 21 d after antigen challenge.

Retroviral transduction

cDNA encoding membrane-bound BAFFR protein was subcloned between the NotI and XhoI sites of the plasmid murine stem cell virus (IRES)–internal ribosome entry site–GFP vector (Gatto et al., 2009), and retroviral particles from empty and BAFFR-expressing vectors were generated using the Phoenix-E packaging cell line together with the pCL-Eco packaging vector as described previously (Swift et al., 2001). For retroviral transduction of SW_{HEL} B cells, spleen cells were harvested and stimulated in vitro with recombinant mouse IL-4 (10 ng/ml; R&D Systems) and anti-CD40 (FGK4.5, 1 µg/ml; BioXcell) in RPMI supplemented with 10% FCS, 55 mM mercaptoethanol, 1 mM sodium pyruvate, 0.1 M nonessential amino acids, 10 mM Hepes, 50 U/ml penicillin, 50 mg/ml streptomycin) for 20 h. Spin transduction of stimulated B cells was then performed with retroviral supernatants in the presence 4 µg/ml polybrene (Sigma-Aldrich) for 4 h and restimulated with medium containing IL-4 and anti-CD40 for a further 20 h. Cells were washed with medium, and the efficiency and effectiveness of transduction were analyzed by flow cytometric analysis of GFP expression and cell surface BAFFR expression.

Statistical analysis

The statistical significance of data was calculated using Prism 8.0 software (GraphPad Software). For comparison between two normally distributed groups, a two-tailed unpaired *t* test with Welch's correction was used. For comparison of more than two parametric datasets, unmatched one-way ANOVA was employed with post hoc multiple comparison using Bonferroni's correction. For comparison of categorical data based on nominal variable significance, the χ^2 contingency test was performed. Confidence levels were set at 99% confidence intervals (CIs), where significance was denoted by P values: *, $P < 0.05$; **, $P < 0.01$; ***, $P < 0.001$; and ****, $P < 0.0001$.

Online supplemental material

Fig. S1 shows the flow cytometry gating strategy for SW_{HEL} donor B cells and the phenotype and numbers of high- and low-affinity GC and MBCs in chimeric mice containing T cells that either do or do not express BAFF. Fig. S2 shows BAFFR expression and B cell numbers in WT versus BAFF-deficient and BAFFR-deficient mice. Fig. S3 shows CD21/CD23 expression profiles in WT and BAFFR-deficient SW_{HEL} B cells before and after depletion of mature B cells, the phenotype and numbers of high- and low-affinity GC B cells, and overall SHM patterns in the GC responses of WT and BAFFR-deficient SW_{HEL} B cells as well as their serum antibody responses. Fig. S4 shows the impact of acute BAFF depletion on naive B cell numbers as well as the early B cell blast, GC, and MBC responses of transferred SW_{HEL} B cells. Fig. S5 shows BAFFR expression and the GC and MBC responses generated from SW_{HEL} B cells transduced with BAFFR-encoding and empty retroviral vectors and the long-term memory and recall responses of WT and TRAF3-deficient SW_{HEL} B cells.

Acknowledgments

We thank the staff of Australian BioResources for animal husbandry, the staff of the Garvan Institute of Medical Research Flow Cytometry Facility for cell sorting, and Clara Young for critical evaluation of the manuscript.

A.W.Y. Lau and V.M. Turner were supported by Australian Postgraduate Research Awards, and T.D. Chan and R. Brink were supported by fellowships from National Health and Medical Research Council of Australia. This work was funded by National

Health and Medical Research Council program grant 1016953.

Author contributions: A.W.Y. Lau designed and performed experiments, interpreted the results, and prepared the manuscript. V.M. Turner designed and performed several experiments. K. Bourne and J.R. Hermes prepared key reagents and helped perform several experiments. T.D. Chan helped with experimental design and research supervision. R. Brink designed experiments, supervised the research, and prepared the manuscript.

Disclosures: The authors declare no competing interests exist.

Submitted: 26 June 2019
Revised: 15 July 2020
Accepted: 3 September 2020

References

Anderson, S.M., M.M. Tomayko, A. Ahuja, A.M. Haberman, and M.J. Shlomchik. 2007. New markers for murine memory B cells that define mutated and unmutated subsets. *J. Exp. Med.* 204:2103–2114. https://doi.org/10.1084/jem.20062571

Barnden, M.J., J. Allison, W.R. Heath, and F.R. Carbone. 1998. Defective TCR expression in transgenic mice constructed using cDNA-based alpha- and beta-chain genes under the control of heterologous regulatory elements. *Immunol. Cell Biol.* 76:34–40. https://doi.org/10.1046/j.1440-1711.1998.00709.x

Benson, M.J., S.R. Dillon, E. Castigli, R.S. Geha, S. Xu, K.-P. Lam, and R.J. Noelle. 2008. Cutting edge: the dependence of plasma cells and independence of memory B cells on BAFF and APRIL. *J. Immunol.* 180:3655–3659. https://doi.org/10.4049/jimmunol.180.6.3655

Chan, T.D., D. Gatto, K. Wood, T. Camidge, A. Basten, and R. Brink. 2009. Antigen affinity controls rapid T-dependent antibody production by driving the expansion rather than the differentiation or extrafollicular migration of early plasmablasts. *J. Immunol.* 183:3139–3149. https://doi.org/10.4049/jimmunol.0901690

Chan, T.D., K. Wood, J.R. Hermes, D. Butt, C.J. Jolly, A. Basten, and R. Brink. 2012. Elimination of germinal-center-derived self-reactive B cells is governed by the location and concentration of self-antigen. *Immunity.* 37:893–904. https://doi.org/10.1016/j.immuni.2012.07.017

Chatham, W.W., D.J. Wallace, W. Stohl, K.M. Latinis, S. Manzi, W.J. McCune, D. Tegzová, J.D. McKay, H.E. Avila-Armengol, T.O. Utset, et al. BLISS-76 Study Group. 2012. Effect of belimumab on vaccine antigen antibodies to influenza, pneumococcal, and tetanus vaccines in patients with systemic lupus erythematosus in the BLISS-76 trial. *J. Rheumatol.* 39:1632–1640. https://doi.org/10.3899/jrheum.111587

Frey, A., J. Di Canzio, and D. Zurakowski. 1998. A statistically defined endpoint titer determination method for immunoassays. *J. Immunol. Methods.* 221:35–41. https://doi.org/10.1016/S0022-1759(98)00170-7

Gardam, S., F. Sierro, A. Basten, F. Mackay, and R. Brink. 2008. TRAF2 and TRAF3 signal adapters act cooperatively to control the maturation and survival signals delivered to B cells by the BAFF receptor. *Immunity.* 28:391–401. https://doi.org/10.1016/j.immuni.2008.01.009

Garside, P., E. Ingulli, R.R. Merica, J.G. Johnson, R.J. Noelle, and M.K. Jenkins. 1998. Visualization of specific B and T lymphocyte interactions in the lymph node. *Science.* 281:96–99. https://doi.org/10.1126/science.281.5373.96

Gatto, D., D. Paus, A. Basten, C.R. Mackay, and R. Brink. 2009. Guidance of B cells by the orphan G protein-coupled receptor EBI2 shapes humoral immune responses. *Immunity.* 31:259–269. https://doi.org/10.1016/j.immuni.2009.06.016

Goenka, R., A.H. Matthews, B. Zhang, P.J. O'Neill, J.L. Scholz, T.-S. Migone, W.J. Leonard, W. Stohl, U. Hershberg, and M.P. Cancro. 2014. Local BLyS production by T follicular cells mediates retention of high affinity B cells during affinity maturation. *J. Exp. Med.* 211:45–56. https://doi.org/10.1084/jem.20130505

Gross, J.A., S.R. Dillon, S. Mudri, J. Johnston, A. Littau, R. Roque, M. Rixon, O. Schou, K.P. Foley, H. Haugen, et al. 2001. TACI-Ig neutralizes molecules critical for B cell development and autoimmune disease: impaired B cell maturation in mice lacking BLyS. *Immunity.* 15:289–302. https://doi.org/10.1016/S1074-7613(01)00183-2

Jacobi, A.M., W. Huang, T. Wang, W. Freimuth, I. Sanz, R. Furie, M. Mackay, C. Aranow, B. Diamond, and A. Davidson. 2010. Effect of long-term belimumab treatment on B cells in systemic lupus erythematosus: extension of a phase II, double-blind, placebo-controlled, dose-ranging study. *Arthritis Rheum.* 62:201–210. https://doi.org/10.1002/art.27189

Kaji, T., A. Ishige, M. Hikida, J. Taka, A. Hijikata, M. Kubo, T. Nagashima, Y. Takahashi, T. Kurosaki, M. Okada, et al. 2012. Distinct cellular pathways select germline-encoded and somatically mutated antibodies into immunological memory. *J. Exp. Med.* 209:2079–2097. https://doi.org/10.1084/jem.20120127

Kräutler, N.J., D. Suan, D. Butt, K. Bourne, J.R. Hermes, T.D. Chan, C. Sundling, W. Kaplan, P. Schofield, J. Jackson, et al. 2017. Differentiation of germinal center B cells into plasma cells is initiated by high-affinity antigen and completed by Tfh cells. *J. Exp. Med.* 214:1259–1267. https://doi.org/10.1084/jem.20161533

Kreuzaler, M., M. Rauch, U. Salzer, J. Birmelin, M. Rizzi, B. Grimbacher, A. Plebani, V. Lougaris, I. Quinti, V. Thon, et al. 2012. Soluble BAFF levels inversely correlate with peripheral B cell numbers and the expression of BAFF receptors. *J. Immunol.* 188:497–503. https://doi.org/10.4049/jimmunol.1102321

Mackay, F., P. Schneider, P. Rennert, and J. Browning. 2003. BAFF AND APRIL: a tutorial on B cell survival. *Annu. Rev. Immunol.* 21:231–264. https://doi.org/10.1146/annurev.immunol.21.120601.141152

MacLennan, I.C., K.M. Toellner, A.F. Cunningham, K. Serre, D.M. Sze, E. Zúñiga, M.C. Cook, and C.G. Vinuesa. 2003. Extrafollicular antibody responses. *Immunol. Rev.* 194:8–18. https://doi.org/10.1034/j.1600-065X.2003.00058.x

Malissen, M., A. Gillet, L. Ardouin, G. Bouvier, J. Trucy, P. Ferrier, E. Vivier, and B. Malissen. 1995. Altered T cell development in mice with a targeted mutation of the CD3-epsilon gene. *EMBO J.* 14:4641–4653. https://doi.org/10.1002/j.1460-2075.1995.tb00146.x

Moran, I., A. Nguyen, W.H. Khoo, D. Butt, K. Bourne, C. Young, J.R. Hermes, M. Biro, G. Gracie, C.S. Ma, et al. 2018. Memory B cells are reactivated in subcapsular proliferative foci of lymph nodes. *Nat. Commun.* 9:3372. https://doi.org/10.1038/s41467-018-05772-7

Pape, K.A., V. Kouskoff, D. Nemazee, H.L. Tang, J.G. Cyster, L.E. Tze, K.L. Hippen, T.W. Behrens, and M.K. Jenkins. 2003. Visualization of the genesis and fate of isotype-switched B cells during a primary immune response. *J. Exp. Med.* 197:1677–1687. https://doi.org/10.1084/jem.20012065

Paus, D., T.G. Phan, T.D. Chan, S. Gardam, A. Basten, and R. Brink. 2006. Antigen recognition strength regulates the choice between extrafollicular plasma cell and germinal center B cell differentiation. *J. Exp. Med.* 203:1081–1091. https://doi.org/10.1084/jem.20060087

Phan, T.G., M. Amesbury, S. Gardam, J. Crosbie, J. Hasbold, P.D. Hodgkin, A. Basten, and R. Brink. 2003. B cell receptor-independent stimuli trigger immunoglobulin (Ig) class switch recombination and production of IgG autoantibodies by anergic self-reactive B cells. *J. Exp. Med.* 197:845–860. https://doi.org/10.1084/jem.20022144

Phan, T.G., D. Paus, T.D. Chan, M.L. Turner, S.L. Nutt, A. Basten, and R. Brink. 2006. High affinity germinal center B cells are actively selected into the plasma cell compartment. *J. Exp. Med.* 203:2419–2424. https://doi.org/10.1084/jem.20061254

Rahman, Z.S.M., S.P. Rao, S.L. Kalled, and T. Manser. 2003. Normal induction but attenuated progression of germinal center responses in BAFF and BAFF-R signaling-deficient mice. *J. Exp. Med.* 198:1157–1169. https://doi.org/10.1084/jem.20030495

Ramsköld, D., I. Parodis, T. Lakshmikanth, N. Sippl, M. Khademi, Y. Chen, A. Zickert, J. Mikeš, A. Achour, K. Amara, et al. 2019. B cell alterations during BAFF inhibition with belimumab in SLE. *EBioMedicine.* 40:517–527. https://doi.org/10.1016/j.ebiom.2018.12.035

Reif, K., E.H. Ekland, L. Ohl, H. Nakano, M. Lipp, R. Förster, and J.G. Cyster. 2002. Balanced responsiveness to chemoattractants from adjacent zones determines B-cell position. *Nature.* 416:94–99. https://doi.org/10.1038/416094a

Sasaki, Y., S. Casola, J.L. Kutok, K. Rajewsky, and M. Schmidt-Supprian. 2004. TNF family member B cell-activating factor (BAFF) receptor-dependent and -independent roles for BAFF in B cell physiology. *J. Immunol.* 173:2245–2252. https://doi.org/10.4049/jimmunol.173.4.2245

Schiemann, B., J.L. Gommerman, K. Vora, T.G. Cachero, S. Shulga-Morskaya, M. Dobles, E. Frew, and M.L. Scott. 2001. An essential role for BAFF in

the normal development of B cells through a BCMA-independent pathway. *Science.* 293:2111–2114. https://doi.org/10.1126/science.1061964

Scholz, J.L., J.E. Crowley, M.M. Tomayko, N. Steinel, P.J. O'Neill, W.J. Quinn III, R. Goenka, J.P. Miller, Y.H. Cho, V. Long, et al. 2008. BLyS inhibition eliminates primary B cells but leaves natural and acquired humoral immunity intact. *Proc. Natl. Acad. Sci. USA.* 105:15517–15522. https://doi.org/10.1073/pnas.0807841105

Shulga-Morskaya, S., M. Dobles, M.E. Walsh, L.G. Ng, F. MacKay, S.P. Rao, S.L. Kalled, and M.L. Scott. 2004. B cell-activating factor belonging to the TNF family acts through separate receptors to support B cell survival and T cell-independent antibody formation. *J. Immunol.* 173: 2331–2341. https://doi.org/10.4049/jimmunol.173.4.2331

Stohl, W., F. Hiepe, K.M. Latinis, M. Thomas, M.A. Scheinberg, A. Clarke, C. Aranow, F.R. Wellborne, C. Abud-Mendoza, D.R. Hough, et al. BLISS-52 and BLISS-76 Study Groups. 2012. Belimumab reduces autoantibodies, normalizes low complement levels, and reduces select B cell populations in patients with systemic lupus erythematosus. *Arthritis Rheum.* 64:2328–2337. https://doi.org/10.1002/art.34400

Suan, D., N.J. Kräutler, J.L.V. Maag, D. Butt, K. Bourne, J.R. Hermes, D.T. Avery, C. Young, A. Statham, M. Elliott, et al. 2017a. CCR6 defines memory B cell precursors in mouse and human germinal centers, revealing light-zone location and predominant low antigen affinity. *Immunity.* 47:1142–1153.e4. https://doi.org/10.1016/j.immuni.2017.11.022

Suan, D., C. Sundling, and R. Brink. 2017b. Plasma cell and memory B cell differentiation from the germinal center. *Curr. Opin. Immunol.* 45: 97–102. https://doi.org/10.1016/j.coi.2017.03.006

Swift, S., J. Lorens, P. Achacoso, and G.P. Nolan. 2001. Rapid production of retroviruses for efficient gene delivery to mammalian cells using 293T cell–based systems. Curr. Protoc. Immunol. May;Chapter 10:Unit 10.17C.

Takemori, T., T. Kaji, Y. Takahashi, M. Shimoda, and K. Rajewsky. 2014. Generation of memory B cells inside and outside germinal centers. *Eur. J. Immunol.* 44:1258–1264. https://doi.org/10.1002/eji.201343716

Tarlinton, D., and K. Good-Jacobson. 2013. Diversity among memory B cells: origin, consequences, and utility. *Science.* 341:1205–1211. https://doi.org/10.1126/science.1241146

Taylor, J.J., K.A. Pape, and M.K. Jenkins. 2012. A germinal center-independent pathway generates unswitched memory B cells early in the primary response. *J. Exp. Med.* 209:597–606. https://doi.org/10.1084/jem.20111696

Thompson, J.S., S.A. Bixler, F. Qian, K. Vora, M.L. Scott, T.G. Cachero, C. Hession, P. Schneider, I.D. Sizing, C. Mullen, et al. 2001. BAFF-R, a newly identified TNF receptor that specifically interacts with BAFF. *Science.* 293:2108–2111. https://doi.org/10.1126/science.1061965

Toellner, K.M., A. Gulbranson-Judge, D.R. Taylor, D.M. Sze, and I.C. MacLennan. 1996. Immunoglobulin switch transcript production in vivo related to the site and time of antigen-specific B cell activation. *J. Exp. Med.* 183:2303–2312. https://doi.org/10.1084/jem.183.5.2303

Toyama, H., S. Okada, M. Hatano, Y. Takahashi, N. Takeda, H. Ichii, T. Takemori, Y. Kuroda, and T. Tokuhisa. 2002. Memory B cells without somatic hypermutation are generated from Bcl6-deficient B cells. *Immunity.* 17:329–339. https://doi.org/10.1016/S1074-7613(02)00387-4

Victora, G.D., and M.C. Nussenzweig. 2012. Germinal centers. *Annu. Rev. Immunol.* 30:429–457. https://doi.org/10.1146/annurev-immunol-020711-075032

Vora, K.A., L.C. Wang, S.P. Rao, Z.-Y. Liu, G.R. Majeau, A.H. Cutler, P.S. Hochman, M.L. Scott, and S.L. Kalled. 2003. Cutting edge: germinal centers formed in the absence of B cell-activating factor belonging to the TNF family exhibit impaired maturation and function. *J. Immunol.* 171:547–551. https://doi.org/10.4049/jimmunol.171.2.547

Warnatz, K., U. Salzer, M. Rizzi, B. Fischer, S. Gutenberger, J. Böhm, A.K. Kienzler, Q. Pan-Hammarström, L. Hammarström, M. Rakhmanov, et al. 2009. B-cell activating factor receptor deficiency is associated with an adult-onset antibody deficiency syndrome in humans. *Proc. Natl. Acad. Sci. USA.* 106:13945–13950. https://doi.org/10.1073/pnas.0903543106

Zuccarino-Catania, G.V., S. Sadanand, F.J. Weisel, M.M. Tomayko, H. Meng, S.H. Kleinstein, K.L. Good-Jacobson, and M.J. Shlomchik. 2014. CD80 and PD-L2 define functionally distinct memory B cell subsets that are independent of antibody isotype. *Nat. Immunol.* 15:631–637. https://doi.org/10.1038/ni.2914

Supplemental material

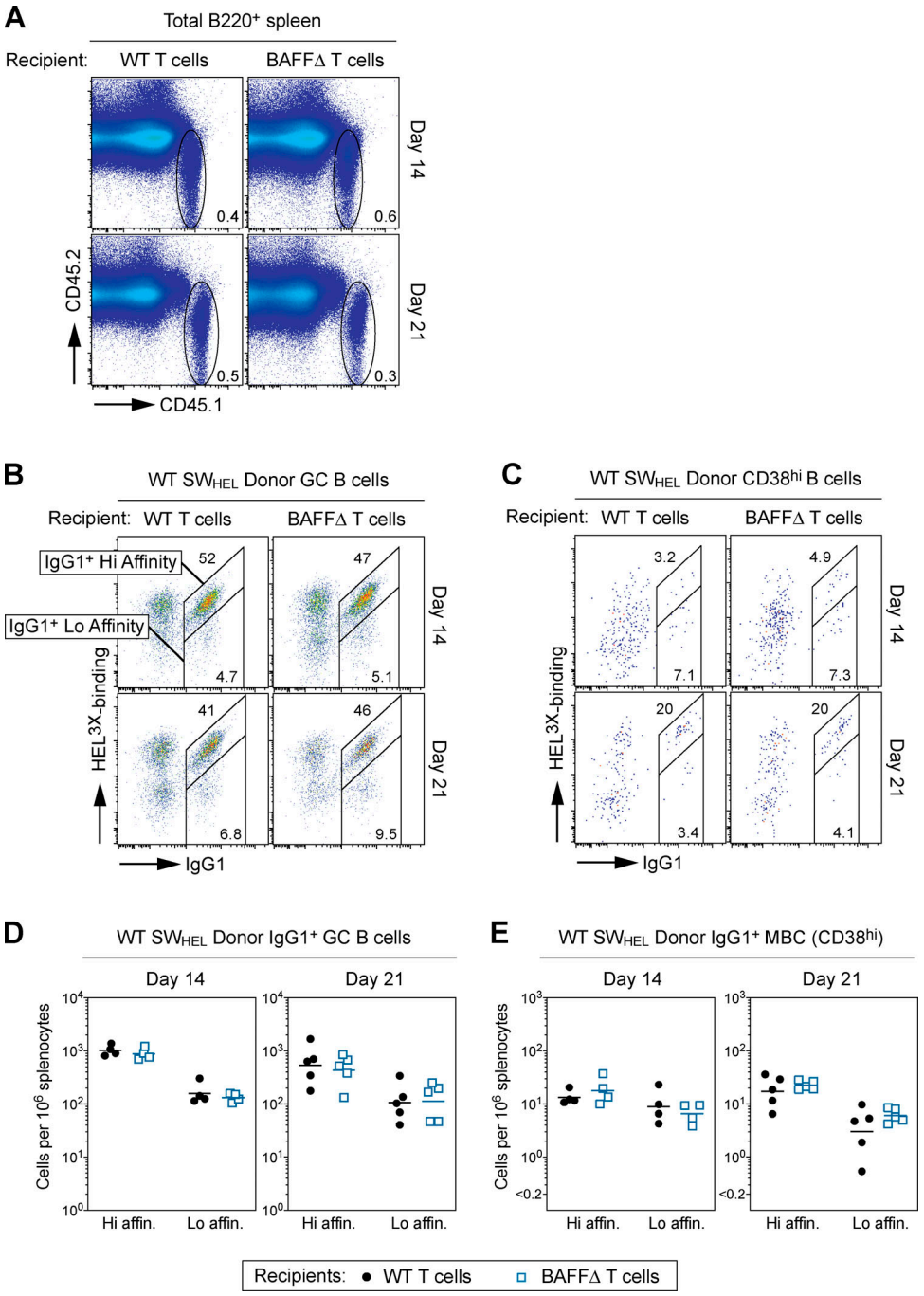

Figure S1. **T cell–derived BAFF does not significantly impact the GC response. (A)** Flow cytometric analysis of total splenic B cells (B220$^+$) in WT T cell and BAFFΔ T cell chimeric recipients, with gate showing donor-derived SW_{HEL} B cells (CD45.1$^+$, CD45.2$^+$) on day 14 (top) and day 21 (bottom). **(B)** Flow cytometric analysis of SW_{HEL} GC B cells (B220^{hi}, CD38^{lo}) in WT T cell and BAFFΔ T cell chimeric recipients, with gates showing IgG1$^+$ HEL^{3X}-binding high- and low-affinity GC compartments on day 14 (top) and day 21 (bottom). **(C)** Flow cytometric analysis of SW_{HEL} CD38^{hi} B cells (B220^{hi}, CD38^{hi}) in WT T cell and BAFFΔ T cell chimeric recipients, with gates showing IgG1$^+$ HEL^{3X}-binding high- and low-affinity MBC compartments on day 14 (top) and day 21 (bottom). Flow data in A–C are representative of five mice from one experiment and are representative of two independent experiments. **(D)** Enumeration of HEL^{3X}-binding high- and low-affinity SW_{HEL} IgG1$^+$ GC B cells and **(E)** SW_{HEL} IgG1$^+$ MBCs on days 14 and 21 in WT T cell and BAFFΔ T cell chimeric recipients. Enumerated data in D and E were analyzed using an unpaired Student's *t* test with Welch's post hoc correction; no statistical significance was found. Data represent five mice from one experiment and are representative of two independent experiments.

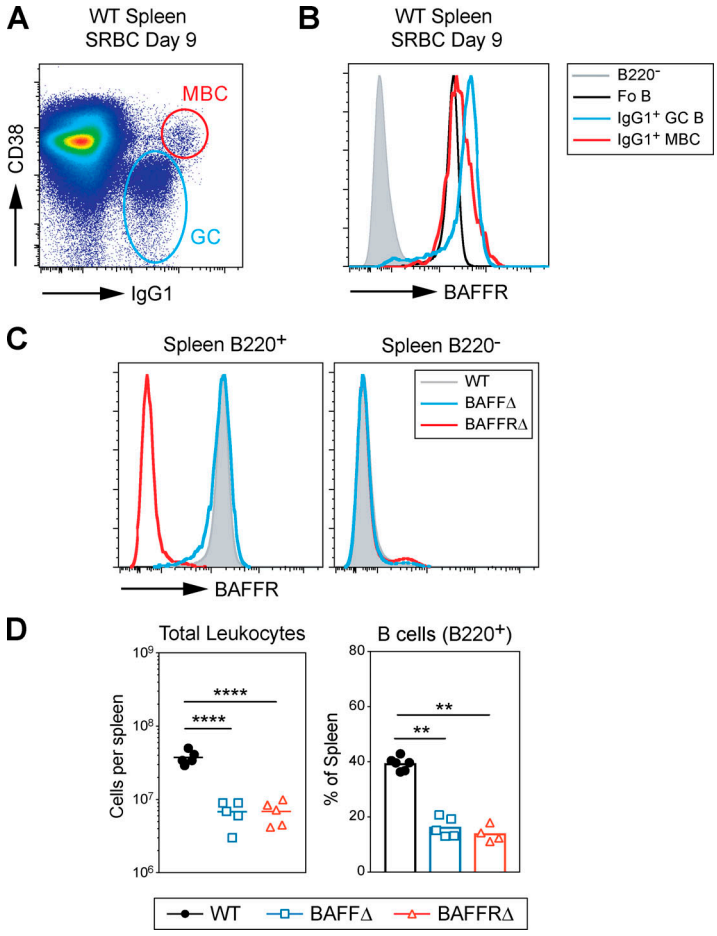

Figure S2. **BAFF is required to support a GC-independent MBC response. (A)** Flow cytometric analysis of splenic B cells ($B220^+$) in SRBC-immunized WT mice, with gates showing $IgG1^+$ GC ($IgG1^+$, $CD38^{lo}$) and $IgG1^+$ MBCs ($IgG1^+$, $CD38^{hi}$) on day 9 after immunization. **(B)** Histogram overlay showing surface BAFFR expression of splenic B cell subsets from day 9 SRBC-immunized WT mice identified in A: non–B cells ($B220^-$; gray), follicular B cells (Fo B; $B220^+$, $CD38^{hi}$, IgD^+; black), $IgG1^+$ GC B cells ($B220^{hi}$, $IgG1^+$, $CD38^{lo}$), and $IgG1^+$ MBCs ($B220^{hi}$, $IgG1^+$, $CD38^{hi}$). **(C)** Histogram overlay showing surface BAFFR expression on splenic B cells ($B220^+$) and non–B cells ($B220^-$) in unimmunized WT (gray), BAFFΔ (blue), and BAFFRΔ (red) mice. Flow data in A–C represent five mice from one experiment and are representative of two independent experiments. **(D)** Quantification of total leukocytes per spleen (left) and percentage of B cells ($B220^+$; right) in spleens of unimmunized WT (black dots), BAFFΔ (blue squares), and BAFFRΔ (red triangles) mice. Enumerated data were analyzed with unmatched one-way ANOVA, with multiple comparison using Bonferroni post hoc correction; **, $P < 0.01$; ****, $P < 0.0001$.

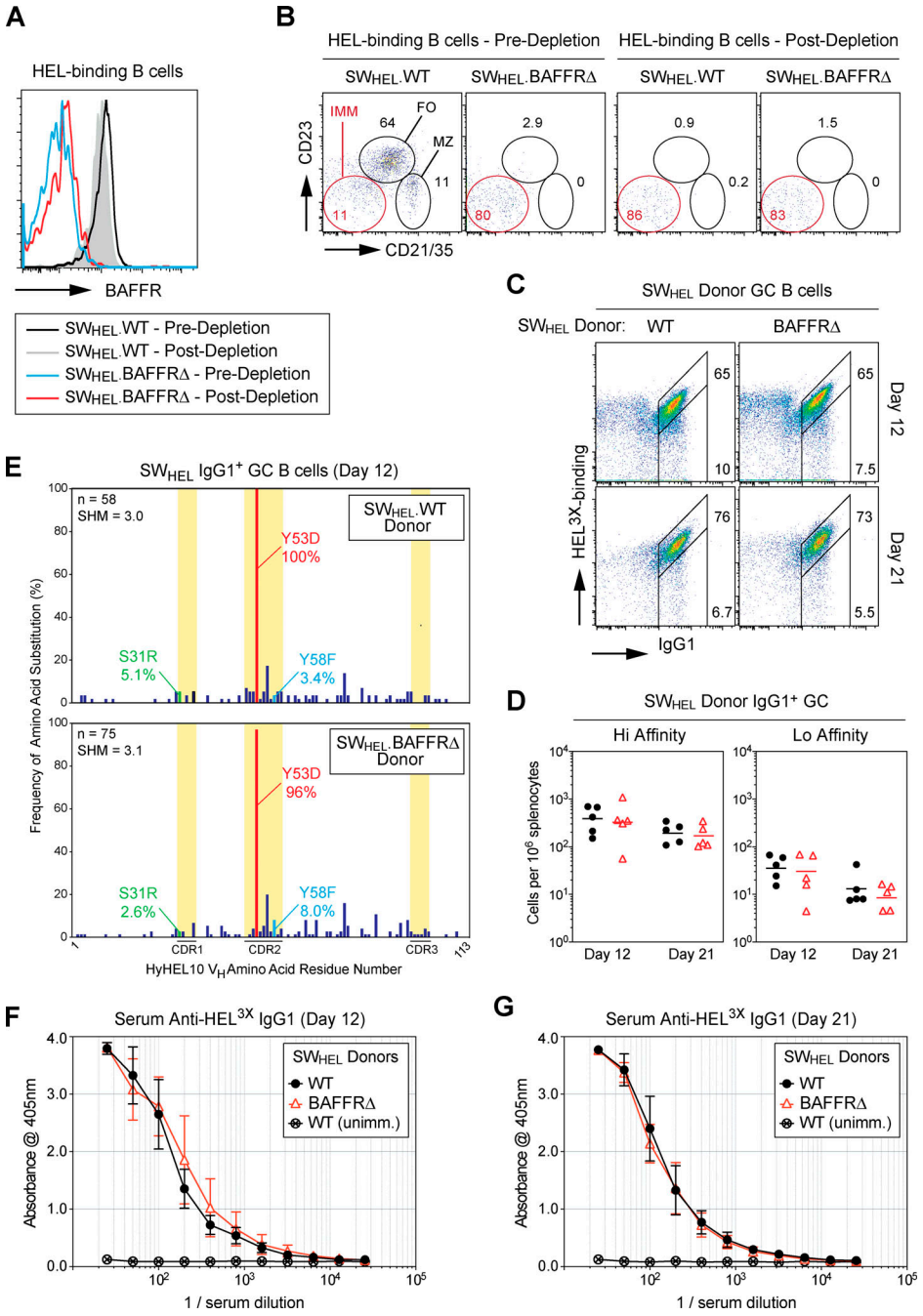

Figure S3. **GC responses progress normally but GC-independent MBC responses are impaired in the absence of BAFFR expression. (A)** Histogram overlay showing surface BAFFR expression of B cells before and after MACS depletion using anti-CD23 and anti-CD35 antibodies: SW_{HEL}.WT B cells before depletion (black) or after depletion (gray) and SW_{HEL}.BAFFRΔ B cells before depletion (blue) or after depletion (red). **(B)** Phenotypic analysis of HEL-binding B cells from SW_{HEL}.WT or SW_{HEL}.BAFFRΔ mice, with gates showing immature B cells ($CD23^{lo}$, $CD21/35^{lo}$), mature follicular B cells ($CD23^{hi}$, $CD21/35^{int}$), and marginal zone B cells ($CD23^{lo}$, $CD21/35^{hi}$) before (left) and after (right) anti-CD23 and anti-CD35 MACS depletion. **(C)** Flow cytometric analysis of donor-derived ($CD45.1^{+}$, $CD45.2^{-}$) WT or BAFFRΔ SW_{HEL} GC B cells ($B220^{hi}$, $CD38^{lo}$), with gates showing $IgG1^{+}$ HEL^{3X}-binding high- and low-affinity compartments in WT recipients on days 12 and 21. Flow data represent five concatenated mice from one experiment and are representative of two independent experiments. **(D)** Enumeration of HEL^{3X}-binding high-affinity (left) and low-affinity (right) SW_{HEL} $IgG1^{+}$ GC B cells from WT (black dots) and BAFFRΔ (red triangles) donors in WT recipient mice. Enumerated data were analyzed using an unpaired Student's *t* test with Welch's post hoc correction. **(E)** SHM analysis of day 12 single-cell–sorted WT (top) or BAFFRΔ (bottom) SW_{HEL} $IgG1^{+}$ GC B cells in WT recipients. Skyscraper plot shows the percentage of mutation at each amino acid residue of SW_{HEL} B cell (HyHEL10) heavy chain variable region V_H10. CDR1, CDR2, and CDR3 are highlighted in yellow. High-affinity mutations to HEL^{3X}: Y53D in red; additional affinity-increasing mutations: Y58F in blue and S31R in green. n = number of clones analyzed; SHM = average number of mutations per clone. SHM data represent five pooled recipient mice from one experiment and are representative of two independent experiments. **(F and G)** Endpoint titration of HEL^{3X}-binding serum IgG1 antibodies on day 12 (F) and on day 21 (G) from WT or BAFFRΔ SW_{HEL} responses detected in WT recipient mice. Serum from unimmunized WT mice (crossed circle) was used as a negative control. ELISA data show geometric mean from five individual mouse in one experiment and are representative of two independent experiments.

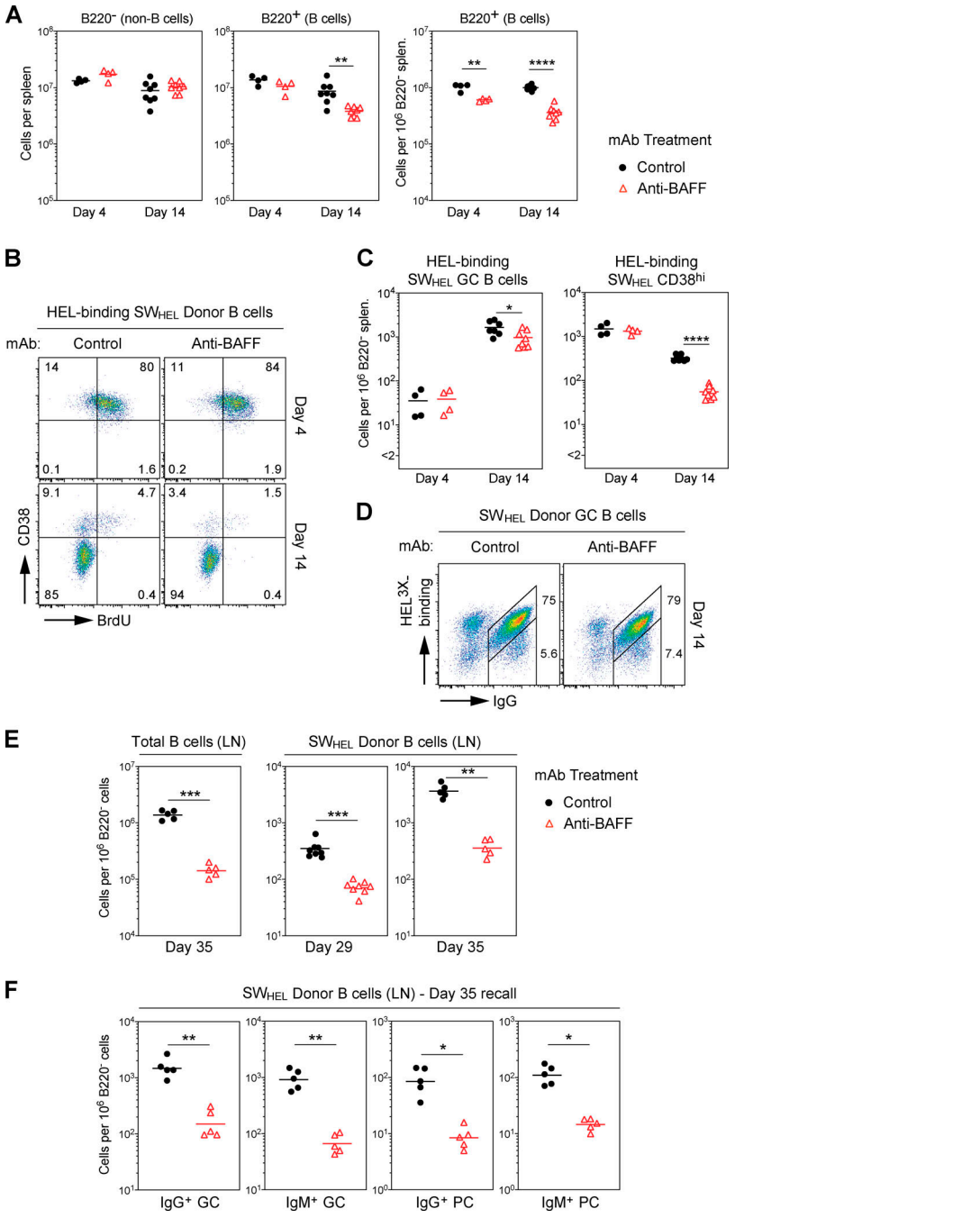

Figure S4. **BAFF dependence of MBC generation and long-term survival. (A)** Enumeration of total splenic non–B cells ($B220^-$; left) and total B cells ($CD45.1^+$, $CD45.2^+$, $B220^+$; center, right) on days 4 and 14 in mice treated with isotype control (black dots) or anti-BAFF (red triangles) antibody. **(B)** Flow cytometric analysis of HEL-binding donor SW_{HEL} B cells ($CD45.1^+$, $CD45.2^-$, $B220^+$, HEL-binding$^+$) on days 4 and 14 in mice treated with isotype control or anti-BAFF antibody. Quadrant gates show the following (from top left): unlabeled naive or activated B cell ($BrdU^-$, $CD38^{hi}$), BrdU-labeled activated B cell and MBC ($BrdU^+$, $CD38^{hi}$), BrdU-labeled GC B cell ($BrdU^+$, $CD38^{lo}$), and unlabeled GC B cell ($BrdU^-$, $CD38^{lo}$) compartments. **(C)** Enumeration of HEL-binding SW_{HEL} GC B cells ($B220^{hi}$, $CD38^{lo}$) and $CD38^{hi}$ B cells ($B220^{hi}$, $CD38^{hi}$) in mice treated with isotype control (black dots) or anti-BAFF (red triangles) antibody. Data in A and C represent four mice on day 4 and eight mice on day 14 from one experiment and are representative of three independent experiments. Enumerated data were analyzed using an unpaired Student's *t* test with Welch's post hoc correction; *, $P < 0.05$; **, $P < 0.01$; ****, $P < 0.0001$. **(D)** Flow cytometric analysis of SW_{HEL} GC B cells ($B220^{hi}$, $CD38^{lo}$), with gates showing $IgG1^+$ HEL^{3X}-binding high- and low-affinity GC compartments on day 14 in recipient mice treated with isotype control or anti-BAFF antibody. Flow data in B and D represent four concatenated mice from one experiment and are representative of three independent experiments. **(E)** Enumeration of primary B cell responses in LNs of mice treated with isotype control (black dots) or anti-BAFF (red triangles) antibody. From left to right: Total LN B cells ($B220^+$) on day 35 and SW_{HEL} B cells ($CD45.1^+$, $CD45.2^-$, $B220^+$) before challenge (day 29) and 5 d after HEL-OVA challenge (day 35). **(F)** Enumeration of recall MBC responses on day 35 in LNs of mice treated with isotype control (black dots) or anti-BAFF (red triangles) antibody. From left to right: SW_{HEL} IgG^+ GC ($B220^{hi}$, IgG^+, $CD38^{lo}$), SW_{HEL} IgM^+ GC B cells ($B220^{hi}$, IgM^+, $CD38^{lo}$), SW_{HEL} IgG^+ PCs ($B220^{lo}$, IgG^+, $CD38^{int}$), and SW_{HEL} IgM^+ PCs ($B220^{lo}$, IgM^+, $CD38^{int}$). Data in E and F represent five replicate mice from one experiment and are representative of two independent experiments. Data were analyzed using an unpaired Student's *t* test with Welch's post hoc correction; *, $P < 0.05$; **, $P < 0.01$; ***, $P < 0.001$.

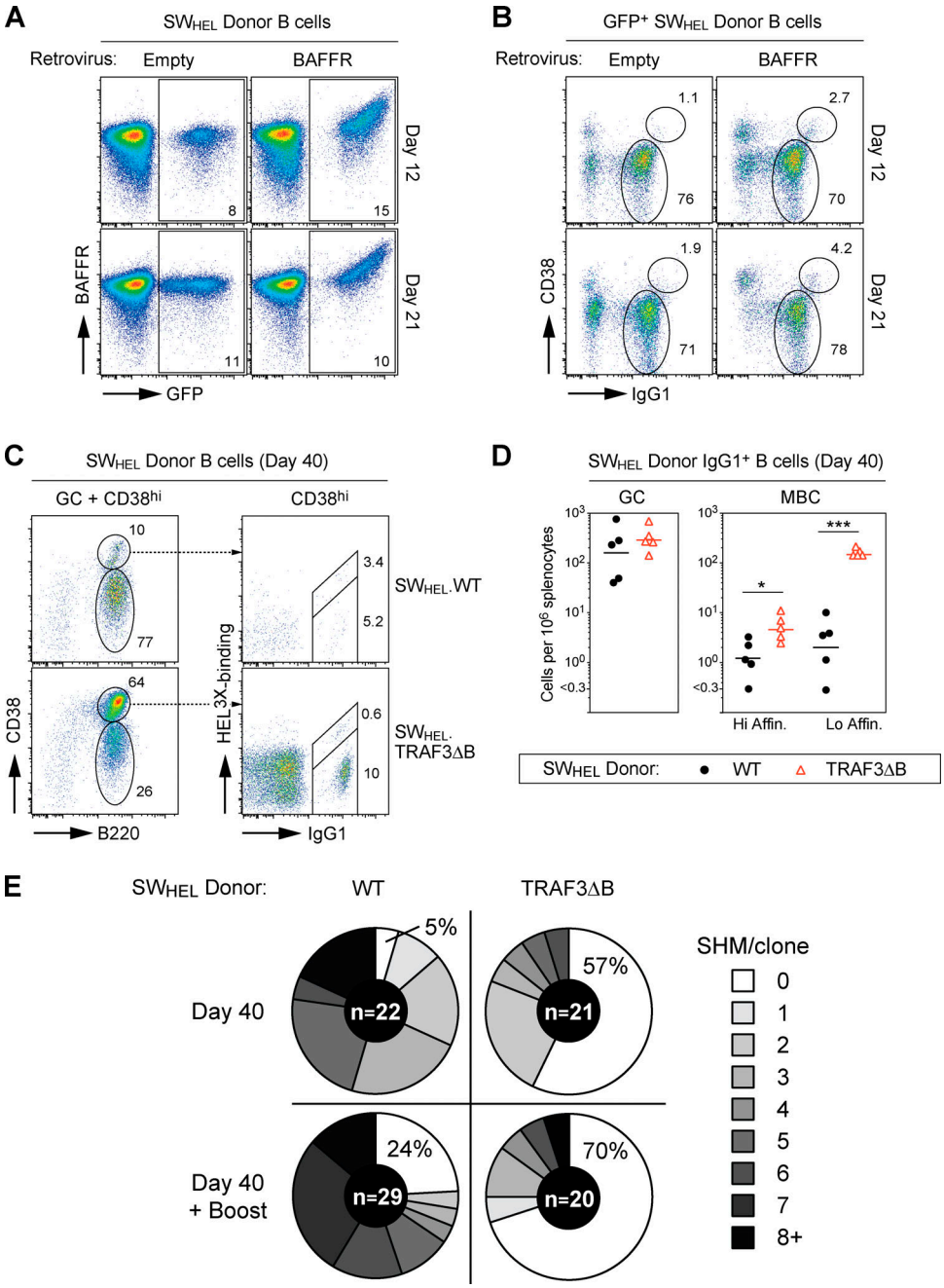

Figure S5. **Increased BAFFR signaling specifically expands GC-independent MBC responses. (A)** Flow cytometric analysis identifying surface BAFFR expression of donor-derived SW_{HEL} B cells (CD45.1$^+$, CD45.2$^-$, B220$^+$) transduced with Empty RV or BAFFR RV (GFP$^+$) and their untransduced counterpart (GFP$^-$) in WT recipient mice on day 12 (top) and day 21 (bottom). **(B)** Flow cytometric analysis of Empty or BAFFR-transduced SW_{HEL} B cells (GFP$^+$, B220$^+$), with gates showing IgG1$^+$ GC B cells (IgG1$^+$, CD38^{lo}) and IgG1$^+$ MBCs (IgG1$^+$, CD38^{hi}) in WT recipient mice on day 12 (top) and day 21 (bottom). Flow data in A and B represent five concatenated mice from one experiment and are representative of three independent experiments. **(C)** WT or TRAF3ΔB SW_{HEL} splenocytes (CD45.1$^+$) were adoptively transferred into WT (CD45.2$^+$) recipients and challenged with HEL^{2X}-SRBC. Recipient mice of WT or TRAF3ΔB donor cells were harvested on day 40 or antigen boosted with HEL^{2X}-HRBC for analysis of the day 5 recall response (day 45). Flow cytometric analysis of WT (top left) or TRAF3ΔB (bottom left) SW_{HEL} donor cells (CD45.1$^+$, CD45.2$^-$), with gates showing GC B cells (B220^{hi}, CD38^{lo}) and CD38^{hi} B cells (B220^{hi}, CD38^{hi}) in WT recipient mice on day 40. SW_{HEL} CD38^{hi} B cells (right panels) were analyzed for IgG1 switching and HEL^{3X} binding, with gates showing HEL^{3X}-binding high- and low-affinity IgG1$^+$ MBC compartments. Flow data represent five mice from one experiment and are representative of three independent experiments. **(D)** Enumeration of WT (black dots) or TRAF3ΔB (red triangles) SW_{HEL} (left) IgG1$^+$ GC B cells (IgG1$^+$, CD38^{lo}) and (right) HEL^{3X}-binding high-affinity (HEL^{3Xhi}) and low-affinity (HEL^{3Xlo}) IgG1$^+$ MBCs (IgG1$^+$, CD38^{hi}) on day 40 in recipients. Enumerated data were analyzed using an unpaired Student's *t* test with Welch's post hoc correction; *, P < 0.05; ***, P < 0.001. **(E)** SHM analysis of single-cell–sorted WT or TRAF3ΔB SW_{HEL} IgG1$^+$ MBCs from primed-only recipients on day 40 (top) and antigen-boosted recipients on day 45 (bottom). Frequency of IgG1$^+$ MBC clones with no mutations in SW_{HEL} B cell (HyHEL10) heavy chain variable region V_H10 (white; SHM/clone = 0) in primed WT donor (5%; top left), primed TRAF3ΔB donor (57%; top right), primed boosted WT donor (24%; bottom left), and primed boosted TRAF3ΔB donor (70%; bottom right). Data represent five recipient mice pooled from one experiment and are representative of three independent experiments. n = number of clones analyzed; SHM/clone = average number of mutations per clone.